Atmos. Chem. Phys. Discuss., https://doi.org/10.5194/acp-2017-1012
Manuscript under review for journal Atmos. Chem. Phys.
Discussion started: 10 November 2017

Atmospheric Chemistry and Physics Discussions

Relationship between Chemical Composition and Oxidative Potential of Secondary Organic Aerosol from Polycyclic Aromatic Hydrocarbons

Shunyao Wang[1], Jianhuai Ye[1], Ronald Soong[2], Bing Wu[2], Legeng Yu[1], Andre Simpson[2], Arthur W.H. Chan[1,*]

[1]Department of Chemical Engineering & Applied Chemistry, University of Toronto

[2] Environmental NMR Centre, Department of Physical and Environmental Sciences, University of Toronto Scarborough

*Correspondence to: Arthur W.H. Chan (arthurwh.chan@utoronto.ca)

Atmos. Chem. Phys. Discuss., https://doi.org/10.5194/acp-2017-1012
Manuscript under review for journal Atmos. Chem. Phys.
Discussion started: 10 November 2017

Atmospheric Chemistry and Physics Discussions

Abstract

Owing to the complex nature and dynamic behaviors of secondary organic aerosol (SOA), its ability to cause oxidative stress (known as oxidative potential, or OP) and adverse health outcomes remain poorly understood. In this work, we probed into linkages between the chemical composition of SOA and its OP, and investigated impacts from various SOA evolution pathways, including atmospheric oligomerization, heterogeneous oxidation and mixing with metal. SOA formed from photooxidation of the two most common polycyclic aromatic hydrocarbons (naphthalene and phenanthrene) were studied as model systems. OP was evaluated using the dithiothreitol (DTT) assay. The oligomer-rich fraction separated by liquid chromatography contributed significantly to DTT activity in both SOA systems (52±10% for NSOA and 56±5% for PSOA). Heterogeneous ozonolysis of NSOA was found to enhance its OP, which is consistent with the trend observed in selected individual oxidation products. DTT activities from redox-active organic compounds and metals were found to be not additive. When mixing with highly redox-active metal (Cu), OP of the mixture decreased significantly for 1,2-naphthoquinone (42±7%), 2,3-dihydroxynaphthalene (35±1%), NSOA (50±6%) and PSOA (43±4%). Evidence from proton nuclear magnetic resonance (^{1}H NMR) spectroscopy illustrates that such OP reduction upon mixing can be ascribed to metal-organic binding interactions. Our results highlight the role of aerosol chemical composition under atmospheric aging processes in determining the OP of SOA, which is needed for a more accurate and explicit prediction of the toxicological impacts from particulate matter.

Atmos. Chem. Phys. Discuss., https://doi.org/10.5194/acp-2017-1012
Manuscript under review for journal Atmos. Chem. Phys.
Discussion started: 10 November 2017

Atmospheric Chemistry and Physics Discussions

1 Introduction

Exposure to particulate matter (PM) has been associated with various adverse health endpoints, such as increased risks of myocardial infarction, ischemic heart disease, lung cancer, exacerbation of asthma, and chronic obstructive pulmonary disease (de Kok et al., 2006; Li et al., 2003a; Li et al., 2003b; Nel, 2005; Risom et al., 2005; Thurston et al., 2016). As a result, ambient $PM_{2.5}$ exposure ranks among the top 5 global mortality risk factors (Cohen et al., 2017). Meanwhile, a decreased ambient PM level has been associated with longer life expectancies (Pope et al., 2009). To establish causal links between aerosol exposure and health endpoints, cytotoxic and carcinogenic potential has been investigated by epidemiological studies in the past decades (Brunekreef and Holgate, 2002; Beelen et al., 2014; Lelieveld et al., 2015; Pope et al., 2002), but the underlying mechanistic pathways by which PM causes adverse health outcomes still remain poorly understood.

Oxidative stress has been proposed as one of the main mechanisms for PM toxicity in recent years, and is often expressed as the oxidative potential (OP) (Li et al., 2003b). OP is the mass normalized capacity of inhaled PM to induce oxidative stress, which is exhibited as redox imbalance through consumption of antioxidants and generation of reactive oxygen species (ROS) (Antiñolo et al., 2015; Shen et al., 2011; Shiraiwa et al., 2012). ROS include a variety of oxidants such as superoxide ($O_2^{\bullet-}$), hydroxyl radical (•OH) and hydrogen peroxide (HOOH), which could either be introduced into human body directly from inhaled PM or generated by targeted cells (Nel et al., 1998; Pöschl and Shiraiwa, 2015; Rhee, 2006; Verma et al., 2015b). The generation of ROS during multiphase interactions between air pollutants and human respiratory tract is closely related to the chemical composition, since the combination of various pollutants may

influence chemical reactivity as well as bioavailability of PM while having synergistic or nonlinear influences on its OP (Antiñolo et al., 2015; Charrier et al., 2015; Fang et al., 2015; Shiraiwa et al., 2012; Xiong et al., 2017).

OP of both organic and inorganic PM components have been evaluated by both cellular and acellular assays. *In vitro* cellular assays were conducted by detecting biological endpoints of the exposure, including heme oxygenase-1 (HO-1) and other cytokines as well as macrophage related biomarker expressions (Krapf et al., 2017; Li et al., 2003b). On the other hand, acellular assays use specific chemicals, such as dithiothreitol (DTT), ascorbate (AA) and glutathione (GSH), as surrogates of low-molecular weight (MW) antioxidants (Fang et al., 2016; Godri et al., 2011;McWhinney et al., 2013). Among acellular assays, the DTT assay quantifies OP by measuring the DTT depletion rate over a fixed time interval, which mimics the physiological process of electron transfer from biological antioxidants to dissolved O_2 (Cho et al., 2005). DTT assay is one of the most commonly used OP evaluation methods, since DTT is a potent surrogate for the total thio-pools (glutathione and protein thiols) while this assay can be conducted under biologically relevant conditions (37 °C, pH=7.4) with relatively simple procedures (Cleland , 1964; Hansen et al., 2009; McWhinney et al., 2011). OP levels measured by this assay have been found to correlate well with cellular ROS expression as well as several airway inflammation biomarkers, such as HO-1, tumor necrosis factor- α (TNF- α) and fractional exhaled nitric oxide (FE_{NO}) (Delfino et al., 2013; Li et al., 2003b; Tuet et al., 2017).

Secondary organic aerosol (SOA) from atmospheric oxidation of gaseous precursors comprises a major fraction of submicron particulate matter. To date, The DTT assay has been applied in a few studies to evaluate the OP of both laboratory and ambient SOA (McWhinney et al., 2013;

Tuet et al., 2017b; Verma et al., 2015a). However, owing to the complex and dynamic property of SOA, there is limited understanding of the relationship between detailed SOA composition and its OP (Charrier and Anastasio, 2012;Pöschl and Shiraiwa, 2015; Tuet et al., 2017b). Tuet et al. (2017b) studied the DTT activity of chamber-generated SOA from both biogenic and anthropogenic VOCs under various conditions, showing that naphthalene SOA (NSOA) has the highest OP. Previous work (Antiñolo et al., 2015; Bolton et al., 2000; Charrier and Anastasio, 2012; Cho et al., 2005; Jiang et al., 2017; Tuet et al., 2017b) indicated while polycyclic aromatic hydrocarbons (PAHs) are unreactive towards DTT while their oxidation products, such as quinones, can be highly redox-active. Quinones can be directly emitted from traffic or formed from secondary oxidation (Cho et al., 2004;McWhinney et al., 2013), and are able to consume antioxidants in a catalytic cycle (Fig. 1) (Bolton et al., 2000;Valavanidis et al., 2005). McWhinney et al.(2013) found three quinones (1,2- naphthoquinone, 1,4-naphthoquinone and 5-hydroxy-1,4-naphthoquinone) in NSOA could only account 30 ±5 % for the observed OP of NSOA, and the source of the remaining DTT activity remains unknown. Peroxides, which are the major contributors to the OP of isoprene SOA (Jiang et al., 2017; Lin et al., 2016; Surratt et al., 2010), may also be abundant in NSOA (Kautzman et al., 2009), but their contribution to the OP of NSOA has not been evaluated. In addition, the composition of SOA may evolve upon atmospheric aging. Previous study (Verma et al., 2009) found ambient samples collected in the afternoon had a larger fraction of water soluble organic carbon and higher OP, suggesting the photochemical aging effects. There may also be correlations between the average carbon oxidation state ($\overline{OS}$c) and OP of SOA at different stages of oxidation (Tuet et al., 2017a). Moreover, mixing between organics and metals was also found to change the OP of specific components in SOA (Xiong et al., 2017), but the mechanisms remain the tip of iceberg.

Here, we focused on understanding how the composition of PAH-derived SOA is related to its strong OP (Tuet et al., 2017b). Specific questions we aim to address in this work are: what are the compounds within SOA that are important for DTT activity? How does the OP change upon atmospheric aging processes, including oligomerization, heterogeneous oxidation, and mixing with transition metals (Gao et al., 2004; Rudich et al., 2007)? In this work, SOA from photoxidation of naphthalene and phenanthrene were studied as model systems, and compared to SOA from ozonolysis of α-pinene and limonene. The relative OP contributions of peroxides and high-MW oligomers were evaluated. Effects of aerosol aging on OP was evaluated by examining the OP of individual oxidation products known to be present in NSOA, and the OP of NSOA samples that were further oxidized in the condensed phase. Lastly, the impacts of SOA mixing with metal was explored by mixing SOA or redox-active SOA components with Cu (II), a transition metal which has been identified with the highest OP in ambient particles (Charrier and Anastasio, 2012). Additivity of OP revealed by DTT assay was investigated, and the mechanisms of Cu-organic interactions were examined in detail using proton nuclear magnetic resonance spectroscopy (^{1}H NMR).

2 Methods

2.1 Flow tube experiments

SOA was produced in a custom-built 10 L quartz flow tube. Details about the flow tube conditions have been described in previous work (Ye et al., 2016; Ye et al., 2017). Prior to each experiment, the flow tube was flushed with purified compressed air at a flow rate of 20 L min^{-1} for over 24 hours.

Atmos. Chem. Phys. Discuss., https://doi.org/10.5194/acp-2017-1012
Manuscript under review for journal Atmos. Chem. Phys.
Discussion started: 10 November 2017

115

116 To produce SOA from naphthalene or phenanthrene, solid PAH was placed in a heated container
117 (80 ℃), and the sublimed vapor was carried into the flow tube in a 0.2 L min^{-1} flow of purified
118 compressed air. O_3 and water vapor were also added into the flow tube. O_3 was produced by
119 passing 0.5 L min^{-1} oxygen (99.6%, Linde, Mississauga, Canada) through an UV O_3 generator
120 (No. 97006601, UVP, Cambridge, UK). Water vapor was produced by bubbling purified air
121 through a custom-made humidifier with a flow rate of 1.3 L min^{-1}. Residence time inside the
122 flow tube was maintained around 5 min. The flow tube was housed inside an aluminum
123 enclosure, which was equipped with 254 nm UV lamps (UVP, Cambridge, UK). The photolysis
124 of O_3 produces O (^{1}D), which react with water vapor to produce •OH and initiate photooxidation
125 of naphthalene/phenanthrene as well as SOA formation. During naphthalene/phenanthrene
126 photooxidation, O_3 concentration inside the flow tube was controlled around 1 ppm. In addition,
127 blank experiments were conducted under the same conditions, without injecting any
128 hydrocarbons.

129

130 Two types of SOA from monoterpene ozonolysis were also synthesized under similar conditions.
131 α-pinene (Sigma-Aldrich, 98%) or limonene (Sigma-Aldrich, 97%) was pre-dissolved in
132 cyclohexane (Sigma-Aldrich, 99.5%) with volumetric ratio of 1:500 or 1:1500, respectively. At
133 these ratios, the reaction rates between •OH and cyclohexane are at least a hundred time higher
134 than that of SOA precursors(Atkinson and Arey, 2003; Keywood et al., 2004). The experimental
135 solution was injected continuously into purified air flow by a syringe (1000 mL, Hamilton)
136 installed on a syringe pump (KDS Legato100) to achieve an initial concentration of 588 ±16 ppb
137 or 298 ±24 ppb of α-pinene or limonene, respectively. O_3 was produced by passing oxygen

through the O_3 generator at a flow rate of 0.2 L min^{-1} or 0.3 L min^{-1} for α-pinene or limonene, respectively, such that the O_3 concentrations were at least 5 times higher than α-pinene or limonene. Both experiments were conducted in the same flow tube without irradiation of UV lights.

Temperature and relative humidity were monitored by an Omega HX94C RH/T transmitter. The concentrations of SOA precursors at the inlet and outlet of the flow tube were measured by a gas chromatography-flame ionization detector (GC-FID, Model 8610C, SRI Instruments Inc., LV, USA) equipped with a Tenax® TA trap. Size distribution and volume concentration of SOA at the flow tube reactor outlet were monitored using a custom-built scanning mobility particle sizer (SMPS), which was composed of a differential mobility analyzer column (DMA, Model 3081, TSI, Shoreview, MN, USA) with flow controls and a condensation particle counter (CPC, Model 3772, TSI, Shoreview, MN, USA). The SMPS data were inverted to particle size distributions using custom code written in Igor Pro (Wavemetrics, Portland, OR, USA). By assuming a particle density of 1.25 g cm^{-3} for monoterpene SOA (Kostenidou et al., 2007; Shilling et al., 2009) and 1.55 g cm^{-3} for PAH SOA(Chan et al., 2009; McWhinney et al., 2011), volume concentrations of particle were converted into mass concentrations and integrated as a function of sample collection time and flow rates to obtain the total mass of collected SOA.

2.2 SOA sampling and extraction

All SOA samples were collected on 47 mm prebaked (500 ℃, 24h) quartz fiber filters (Pall, Ann Arbor, MI, USA) in a stainless-steel filter holder after reaching a steady state yield, and then wrapped in prebaked aluminum foil before being stored in sterile petri dishes sealed with

Atmos. Chem. Phys. Discuss., https://doi.org/10.5194/acp-2017-1012
Manuscript under review for journal Atmos. Chem. Phys.
Discussion started: 10 November 2017

Parafilm M® at -20 ℃. Within 3 days of collection, the filters were extracted in methanol (HPLC grade, 99.9%, Sigma Aldrich, St. Louis, MO, USA), by ultra-sonication at room temperature for more than 3 minutes. After sonication, insoluble materials were filtered by a PTFE (polytetrafluoroethylene) syringe filters (Fisherbrand™) with pore size of 0.22 μm. Chemical analysis and DTT activities of the filter extracts were conducted within hours after extraction. As negative control, filter samples were also collected during blank experiments and extracted in the same manner.

2.3 DTT assay

OP of SOA and selected quinone/peroxide standards were quantified by the depletion rate of DTT, an antioxidant that can be consumed by oxidative components in PM (Kumagai et al., 2002). The protocols used in this work are adapted from those of McWhinney et al.(2011; 2013). The SOA extracts were first evaporated to complete dryness in a 5.0 L min^{-1} of N_2 using a blow-off system (N-EVAP, Organomation, USA). Phosphate buffer (0.1 M, pH 7.4) was then added to dissolve the SOA to achieve a concentration of 0.2 mM. For quinones, copper(II) sulfate and peroxides, each pure compound was weighed and dissolved in 0.1 M phosphate buffer. The concentration of quinones and copper (II) sulfate solutions was 1 μM, and the concentration of each peroxide solution was 100 μM. The specific solution was then added into multiple wells in a 96-well UV plate (Greiner Bio-One, Kremsmünster, AT), and immediately covered with adhesive plate sealer (EdgeBio, Gaithersburg, USA). The plate was then placed in a UV-Vis spectrophotometer (Spectramax 190, Molecular Devices Corporation, Sunnyvale, CA) for incubation. The incubation temperature was maintained at 37 ℃ inside the spectrophotometer to mimic human physiological conditions. 0.02 ml DTT was then added into each well to initiate

the redox-reactions. At each time point, 0.02 ml of 5, 5'-dithiobis (2-nitrobenzoic acid) (DTNB) was added, which immediately consumed all the remaining DTT to form a yellow product, 2-nitro-5-thiobenzoic acid (TNB) (Fig.S1). TNB was quantified by the light absorption at a wavelength of 412nm, which was further converted to the DTT amount by calibration curve (Fig. S2b) in order to obtain the DTT decay rate. The reaction was quenched by adding DTNB at different wells at different times (all containing the same initial mixture), allowing for quantification of the DTT decay rate over a 30 minute time interval (every 5 minutes for the first 10 minutes and then every 10 minutes). Blank control and the calibration curve for DTT quantification are shown in Fig. S2. Here, we used the total DTT decay rate, DTT_t (μM DTT min^{-1}), to report the total oxidative capacity, as well as the mass normalized DTT decay rate, DTT_m (pmol DTT $min^{-1}\mu g^{-1}$ organics), to report the OP (Charrier et al., 2016; Jiang et al., 2017; Xiong et al., 2017). Detailed information about the chemicals used in this assay is shown in section S1.

2.4 Quantification of peroxides in SOA

Quantification of total peroxides in the four types of SOA was conducted using the iodometric-spectrophotometric method, which quantifies total aerosol peroxides in all three forms (H_2O_2, ROOH, ROOR) (Banerjee and Budke, 1964;Docherty et al., 2005):

$$ROOR + 2I^- + 2H^+ \rightarrow 2ROH + I_2 \quad (1)$$

$$I_2 + I^- \rightarrow I_3^- \quad (2)$$

where I^- is oxidized to I_2 by peroxides under acidic conditions, and then complexes with remaining I^- to form I_3^-, a compound with brown color detected spectrophotometrically at a wavelength of 470nm. The concentration of each SOA solution was first adjusted to 5mM. 0.02

ml of potassium iodide solution (1 g ml^{-1}, KI dissolved in DI water), which provided the I^- in reaction (1), and 0.02 ml of formic acid (≥95%), which maintained the acidity, were added to 0.16 ml of the SOA solution in each well of a 96-well UV plate. The plate was immediately sealed and incubated for 1 h following the same procedures as in the DTT assay, and the UV-vis absorbance was measured at 470 nm. After testing for the sensitivities of various peroxides in KI assay (Fig. S3), and following the previous work by Kautzman et al.(2009), benzoyl peroxide (≥98%) was chosen to represent peroxides in NSOA and used as standards for mass calibration in this study. All values are reported as mass fraction of peroxides in the total SOA.

2.5 Heterogeneous oxidation

Heterogeneous oxidation of NSOA was conducted by first cutting a filter with freshly collected NSOA into halves (within 3 days of flow tube synthesis and stored at -20 ℃). One half of the filter was placed in a sealed container, and an O_3 stream (~3ppm, from the previously mentioned O_3 generator) was passed through the filter at a flow rate of 0.2 $Lmin^{-1}$. The other half of the filter was treated in parallel with a 0.2 L min^{-1} flow of N_2 over the same time intervals, to account for evaporation and/or decomposition of SOA components at room temperature. 3 sets of experiments were conducted with exposure times of 1 h, 12 h and 24 h where the O_3 exposure can be determined by,

$$O_3 \text{ exposure} = \int_0^t [O_3]\, dt = \langle O_3 \rangle_t \times t \quad (3)$$

where $\langle O_3 \rangle_t$ is the time averaged O_3 concentration at a total flow rate of 0.2 L min^{-1}. The DTT activity of each O_3-exposed aerosol sample was normalized to that of the corresponding N_2 exposure group. Changes in organic carbon mass on NSOA filters exposed to O_3/N_2 for 1h, 12h

and 24h were also monitored with a thermal optical organic carbon/elemental carbon (OC/EC) aerosol analyzer instrument (Sunset Laboratory Inc., Tigard, OR, USA). OC/EC content was measured following the IMPROVE OC/EC protocol (Chow et al., 1993). Blanks were measured before each run and subtracted from the sample measurements.

2.6 Chromatographic Separation of NSOA

To identify the relative contributions of monomers and oligomers in N/ PSOA to DTT activity, the SOA extract was separated using ultra-high performance liquid chromatography (UHPLC), and analyzed using electrospray ionization/Ion Mobility-Time of Flight Mass Spectrometry (ESI/IMS-TOF MS, TOFWERK, Switzerland, hereafter referred to as IMS-TOF). SOA methanol extract (30 g L^{-1}) was separated on a reverse phase column (ZORBAX Eclipse Plus C18, Agilent, USA) with an initial mobile phase of 90% DI water and 10% HPLC methanol at a flow rate of 0.15ml min^{-1} (1290 Infinity II, Agilent, USA). The ratio of water to methanol was gradually adjusted from 9:1 to 1:9 between 25 and 30 min. Separation temperature was set to 30 ℃ with a pressure setting of 150 bar. The outlet flow was regulated using a LC-MS post column flow splitters (Supelco, SigmaAldrich, USA) at a ratio of 30:1. The major flow was collected in two different fractions: the first fraction was collected between 6 and14 min, and the second fraction was collected between 14 and 33 min for NSOA (3-17min and 17-28min for PSOA). DTT assay was conducted on each fraction to assess their OPs. The minor flow injected into IMS-TOF was controlled at 5ul min^{-1} for mass spectrometric analysis in the negative mode.

A deactivated fused silica capillary (360µm OD, 50 µm ID, 50cm length, New Objective, Woburn, MA, USA) was used as the sample transfer line between the UHPLC and the IMS-TOF.

253 The ESI source was equipped with an uncoated SilicaTip Emitter (360µm OD, 50 µm ID, 50 µm
254 tip ID, New Objective, Woburn, MA, US). Charged SOA droplets generated from the tip of the
255 emitter were transferred through a desolvation region by a 1L min^{-1} N_2 flow at room temperature,
256 and ions produced from the evaporated droplets were introduced into the drift tube for ion
257 mobility separation. The IMS drift voltage was set to –1.2 kV for the negative mode. The
258 separation temperature was set to 80±1◦C with an operation pressure setting of 1.2 bar for the
259 whole mass spectrometer. After separation in the ion mobility region, the ion *m/z* is measured by
260 high-resolution time-of-flight mass spectrometry within an *m/z* range of 40 to 800. Resolution
261 (m/dm50) of the time-of-flight mass spectrometer is typically 3500–4000 FWHM at *m/z* 250
262 (Groessl et al., 2015; Krechmer et al., 2016). Spectra recording and data processing of the current
263 study were performed using routines written in Igor Pro (6.37, Wavemetrics, OR, USA):
264 "Acquility" (version 2.1.0, http://www.tofwerk.com/acquility) for raw data acquisition and
265 "Tofware" (version 2.5.3, www.tofwerk.com/tofware) for post processing.
266
267 **2.7 ^{1}H NMR spectroscopy**
268 ^{1}H NMR spectroscopy was used to further investigate the mechanism behind the OP reduction
269 upon mixing specific organics and transition metals (Simpson et al., 2011;Simpson and Simpson,
270 2014; Smith and van Eck, 1999). NMR measurements were performed on a Bruker Avance III
271 NMR spectrometer (11.7 T), equipped with a 4 channel liquid state (^{1}H, ^{13}C, ^{15}N, ^{2}H) inverse
272 detection probe (QXI) fitted with an actively shielded Z gradient. Typical parameters used for
273 1D ^{1}H experiments were: a 9.5 µs ^{1}H pulse, 64k acquisition points, 14 ppm spectral width and 8
274 transients were collected, with a total of 5.7s between scans. Before NMR analysis, each sample
275 was dissolved into deuterium oxide (D_2O, Cambridge Isotope Laboratories, 99.96 %) and

dimethyl sulfoxide (DMSO, Fisher Scientific, 99.9 %) at a ratio of 9:1. Here we used D_2O as a lock reagent by suppressing it through pre-saturation.

In order to monitor the duration for the nuclear spin magnetization returning to an equilibrium state, NMR relaxation times T1(longitudinal direction), T2 (transverse direction) were analyzed. T1 of the sample was measured through the standard inversion recovery experiment. The delay periods used for T1 measurements ramped from 0.001 s to 15s in 16 increments with a delay of 60s between scans, which represented > 5 x T1 time to permit full signal recovery. For each delay period, 16 transients were collected. The T2 of the sample was measured through the standard Carr-Purcell-Meiboom-Gill (CPMG) sequence. The delay periods used for T2 measurements ramped from 1.2ms to 614ms in 16 increments with a delay of 60s between scans, which represented > 5 x T1 time to permit full signal recovery. For each delay period, 16 transients were collected. A total of 16 free induction decays were collected for each of the relaxation experiments, and relaxation time calculations were done on Bruker Dynamics Centre (v 2.4.5) using mono-exponential fitting functions (Eq. 3 and 4 below).

$$f(t) = I_0 \times [1 - 2e^{-t/T1}] \quad (4)$$

$$f(t) = I_0 \times e^{-t/T2} \quad (5)$$

Eq. (4) and Eq. (5) are the fitting functions for T1 and T2, respectively, where "I_0" is the thermal equilibrium state of the overall proton nuclear spin magnetization; "t" is the variable delay time. All the ^1H NMR spectra were collected using TopSpin (Bruker, v 3.2). Post-NMR-data processing was conducted in MestReNova (Mestrelab Resesarch, v 11.0.4) and Origin (OriginLab, v 9).

Atmos. Chem. Phys. Discuss., https://doi.org/10.5194/acp-2017-1012
Manuscript under review for journal Atmos. Chem. Phys.
Discussion started: 10 November 2017

299 **2.8 Statistical analysis**

300 Data in this study were interpreted as mean ±standard error of the mean (SEM, n=3), and
301 significance analyses among DTT activities were performed by Student's t-test with a 95%
302 confidence interval. A statistical value of $p < 0.05$ was considered significant.

303

304 **3 Results and discussion**

305 **3.1 DTT activity of laboratory generated SOA**

306 Here, we chose two types of SOA derived from PAHs, naphthalene and phenanthrene, as the
307 model SOA systems. The OP of NSOA has been shown to be the highest among various types of
308 SOA previously studied (Tuet et al., 2017a;Tuet et al., 2017b). At the same time, both NSOA
309 and PSOA contain quinones which are known to be highly redox active and exhibit high OP
310 (Cho et al., 2004; McWhinney et al., 2013). As a comparison, α-pinene and limonene SOA from
311 ozonolysis were chosen to represent biogenic SOA derived from monoterpenes. Experimental
312 conditions and SOA yield information are summarized in Table 1.

313

314 The mass-normalized DTT decay rate, DTTm, was applied here for OP evaluation (Fig. 2).
315 Similar DTTm have been reported for NSOA, with values of 118 pmol $min^{-1}\mu g^{-1}$ by McWhinney
316 et al. (2013) and 110 pmol $min^{-1}\,\mu g^{-1}$ by Tuet et al. (2017b) for NSOA generated from chamber
317 photooxidation under dry conditions. The DTTm of α-pinene SOA of 19.1 ±2.5 pmol $min^{-1}\,\mu g^{-1}$ in
318 this study is also consistent with those reported by Tuet et al.(2017b) and Jiang et al.(2017). The
319 similar values among the different studies highlight the reproducibility of results from the DTT
320 assay. To the best of our knowledge, the OP of PSOA and limonene SOA from this study are the
321 first ones reported in the literature. Both SOA derived from PAHs yield a higher OP than the two

types of monoterpene SOA. The similarities in OP between limonene and a-pinene SOA (cyclic monoterpenes), and between naphthalene and phenanthrene SOA (PAHs) observed in this study further confirms the hypothesis proposed by Tuet et al.(2017b) that the intrinsic OP of SOA is closely related to the molecular skeleton of the precursor.

One of the reasons for the high OP exhibited by PAH-derived SOA is the abundance of redox-active quinone moieties in SOA compounds (Lee and Lane, 2009). The cytotoxic and carcinogenic effects from quinone-like compounds are well recognized in the field of biochemistry (Bolton et al., 2000; Valavanidis et al., 2005), and the toxicity of PM has been attributed to the presence of quinones. Charrier and Anastasio (2012) have found the OP of several quinones are comparable to transition metals in ambient particles. The importance of quinone-like components to OP was also evaluated by examining the changes in DTT activity in response to the presence of 2,4-dimethylimidazole, which has been shown to be the co-catalyst of the quinone redox cycle (Jiang et al., 2017). However, McWhinney et al. (2013) quantified three quinones in NSOA using GC/MS and found that these quinones can only account for 30% of the total NSOA DTT response. The remaining DTT activity may arise from other quinone-like compounds that have not been identified, or from other oxidation products in NSOA. Given this knowledge gap, we examine the potential roles of peroxides, oligomers and other more oxygenated products that may explain the high DTT activities of NSOA in the next sections.

3.2 OP contribution from peroxides

One of the main hypothesis in this study is that organic peroxides contribute to OP. Organic peroxides have been identified to be major components in both laboratory and ambient OA

(Jokinen et al., 2014; Lin et al., 2016; Surratt et al., 2010; Zhang et al., 2015; Zhang et al., 2017). They can play important roles in forming high-MW oligomers (Docherty et al., 2005) and highly oxygenated molecules (Mentel et al., 2015). Recent studies have shown that peroxides may also be important for OP. Kramer et al. (2016) suggested that isoprene-derived hydroxyhydroperoxide (ISOPOOH) is an essential contributor to the OP of isoprene SOA, consistent with the results of bulk peroxide measurements using 4-nitrophenylboronic acid assay (NPBA assay) by Jiang et al. (2017). Since peroxides have been proposed to be a major component in NSOA (Kautzman et al., 2010), it is essential to determine whether or not these peroxides can account for the remaining OP contribution (McWhinney et al., 2013).

Here we compare the NSOA and α-pinene SOA systems to determine the role of peroxides in OP. The KI assay is known to be sensitive to all types of SOA peroxides (ROOR, ROOH and HOOH) (Banerjee and Budke, 1964), and we confirmed its sensitivity by conducting calibrations with 4 different peroxides (Fig. S3). Similar KI response factors were observed with hydrogen peroxide, cumene hydroperoxide, tert-butyl peroxide and benzoyl peroxide. Since it is likely that the peroxides in NSOA have one aromatic ring are mostly in the form of ROOR (Kautzman et al., 2009), we used benzoyl peroxide as the mass calibration standard. The mass fraction of peroxides and DTTm of each SOA system are shown in Table 2. A high percentage of peroxide (40-100%) was observed in α-pinene SOA, which was consistent with the results (47%) in the study by Docherty et al. (2005). Meanwhile, a very low percentage of peroxides (<3%) was found in NSOA system, a result that is inconsistent with previous work (>20%) by Kautzman et al. (2009). The difference in measured peroxide content is most likely due to the difference in the UV light source. Kautzman et al. (2009) and McWhinney et al. (2013) used H_2O_2 photolysis

under black lights (~350 nm), whereas in our study 254 nm UV lamps were used to photolyze O_3 and generate O (^{1}D). Organic peroxides in SOA are known to be photo-labile (Banerjee and Budke, 1964; Krapf et al., 2016; Wang et al., 2011) and had likely decomposed rapidly under the shorter UV wavelengths used in our studies. Despite the differences in light conditions and peroxide content, the DTTm measured for NSOA in this study is consistent with those measured in two separate studies (McWhinney et al., 2013; Tuet et al., 2017). Also, the DTT_m of NSOA was found to be significantly higher than that of α-pinene SOA, which contains a large fraction of peroxides. Therefore, from our work, there is no evidence showing that peroxides contribute significantly to the high DTT_m observed in NSOA. Even if organic peroxides were present at a mass fraction of around 20%, as reported by Kautzman et al., (2010), we expect these peroxides would react with DTT at a similar rate as benzoyl peroxide, which has a similar structure that the proposed peroxides. The DTTm of benzoyl peroxide (ROOR-type) is 38 pmol $min^{-1}ug^{-1}$, which is around 3 times lower than the DTTm of NSOA. It should also be noted that organic hydroperoxides are the major OP contributors for biogenic SOA, such as isoprene and monoterpene SOA (Jiang et al., 2017). One of the potential mechanisms is the formation of hydroxyl radicals from the decomposition of organic hydroperoxides in water (Tong et al., 2016). For the NSOA system, our results suggest that other non-peroxide species are likely to serve as major contributors to OP.

3.3 OP of oligomers in NSOA

Atmospheric OA also undergoes extensive oligomerization, forming high-MW compounds that have profound impacts on SOA physicochemical properties (Hallquist et al., 2009; Rudich et al., 2007; Trump and Donahue, 2014;Wang et al., 2011). Laboratory photooxidation of aromatic

391 compounds produces a substantial fraction of oligomers in the SOA (Kalberer et al., 2004) and
392 these oligomers may be highly functionalized (Gao et al., 2004; Tolocka et al., 2004;). IMS-TOF
393 analysis reveals that a substantial fraction of the signals in NSOA and PSOA are located in the
394 high *m/z* range, which are associated with high-MW oligomeric products. Since previous studies
395 have largely focused on monomeric quinones (such as 1,2-naphthoquinone or 9,10-
396 phenanthrenequinone), the contribution of high-MW products to OP have not been studied and
397 may explain the "missing" OP contributors.
398
399 To evaluate OP of high-MW products in NSOA and PSOA, solutions of SOA extract were
400 separated in a C18 reverse phase column into two major fractions. As shown in Fig. 4, when
401 analyzed by IMS-TOF, the first fraction was found to contain relatively higher signals at *m/z*
402 associated with monomers, and the second fraction contain products with higher signals located
403 in a higher *m/z* range. It should be noted that complete separation could not be achieved in this
404 work. Other techniques, such as size exclusion chromatography (Di Lorenzo and Young,
405 2016;Di Lorenzo et al., 2017), may yield better separation based on molecular weights, but may
406 not be able to resolve compounds in the relative low molecular weight range in the current study.
407 Nonetheless, the first fraction can be qualitatively described as a "monomer-rich" fraction, and
408 the second fraction can be regarded as an "oligomer-rich" fraction (Fig. 4, Fig. 5a, b). The DTT
409 assay was then conducted on both of the original SOA solution as well as the two separated
410 fractions. Since the amount of organic material in each fraction is not known, we use the total
411 DTT activity (DTTt, in μM min^{-1}) to qualitatively compare the oxidative capacities of the two
412 fractions.
413

As shown in Fig. 5, both the monomer-rich and oligomer-rich fractions are reactive towards DTT. For NSOA, the OP contribution from the monomer-rich fraction and the oligomer-rich fraction were 16±3% and 56±10%, respectively (Fig. 5c). For PSOA, the OP contribution from the monomer-rich fraction and the oligomer-rich fraction were 40±8% and 50±5%, respectively (Fig. 5d). In both systems, the oligomer-rich fraction caused a more rapid decay in DTT than the monomer-rich fraction even with a lower summed ion signal of low-MW constituents (Fig. 5a, b for NSOA and PSOA, respectively). These qualitative results suggest that while the current focus of health studies has been focused on monomeric quinones, other higher-MW products may be important for the OP of NSOA and PSOA. Specific molecular characteristics of these high-MW OP contributors are currently unknown, and understanding them will be the subject of future research. It is very likely that the oligomers also contain redox-active quinone functional groups, such as those formed on the surface of oxidized soot (Antiñolo et al., 2015), and are therefore important for OP.

3.4 OP from heterogeneous oxidation

In addition to its complexity, the composition of SOA is also highly dynamic and evolves upon atmospheric oxidation (Jimenez et al., 2009). Heterogeneous oxidation in the particle phase is one of the major pathways in aerosol aging (George and Abbatt, 2010;Rudich et al., 2007) and can increase oxygen content during the functionalization processes. McWhinney et al. (2013) attributed 21% of the NSOA's DTT activity to two quinone isomers (1,2-NQN and 1,4-NQN) in NSOA while found a higher DTT contribution (30%) when they took 5-hydroxy-1,4-naphthoquinone (5-OH-1,4-NQN) into consideration. Thus, we expect that oxygenated

436 derivatives produced upon heterogeneous oxidation may also contribute to the OP of SOA, and
437 the OP of SOA could be enhanced by heterogeneous oxidation.
438
439 We first examined the changes in OP with additional functional groups in known organic
440 compounds. As shown in Fig. 6, two pairs of organic compounds in NSOA were chosen: 1,4-
441 NQN, and 5-OH-1,4-NQN were used to study quinone-like compounds while naphthol (NPL)
442 and 1,3-dihydroxy naphthalene (1,3-DHN) were used to compare phenol-like compounds. The
443 $\overline{OS}$c of those four components were calculated (Kroll et al., 2011), as shown in Fig.6. Our results
444 demonstrated a higher DTTm for standards with higher oxidation states. For each addition of an
445 OH group to the selected molecule, the OP increases. OP of an aromatic compound is therefore
446 shown here to be associated with its degree of oxygenation and is demonstrated here
447 fundamentally using individual organic compounds.
448
449 More broadly, oxidation also increases the degree of oxygenation in the bulk aerosol phase, and
450 increases OP. Here we conducted heterogeneous oxidation by exposing filter-collected SOA to
451 O_3/ N_2 with the same flow rate. The N_2 exposure group is used as the control group in order to
452 isolate the effects of evaporation and/or decomposition at room temperature from those of
453 heterogeneous O_3 oxidation. For each of the exposure (1h, 12h, 24h), the DTTt of O_3 exposure
454 group was normalized by the DTTt of the corresponding N_2 exposure group (Fig.7a). OC loss
455 was determined by thermal optical OC/EC analysis, and was observed to be 17% and 13% for
456 the O_3 and N_2 exposure groups after 24 hours, respectively (Fig.7b). Generally, DTTt of NSOA
457 filter under O_3 exposure was higher than that of N_2 exposure. The study of Antiñolo et al.(2015)
458 also showed an increased redox activity of soot accompanied by an increased amount of

459 oxygenated derivatives (quinone) under heterogeneous oxidation. However, the enhanced
460 oxidative capacity from heterogeneous ozonolysis appeared to decrease with longer exposure to
461 O_3 (Fig.7a), which we hypothesize may result from functionalization as well as fragmentation of
462 organic molecules during heterogeneous oxidation (Kroll et al., 2009). This can be further
463 confirmed with the observed changes in the different OC fractions, as shown in Fig. S4. Within
464 the 24h exposure, the volatile fractions (OC1 and OC2) of the O_3 exposed group increased while
465 the less volatile fractions (OC3 and OC4) decreased compared to the N_2 group, which suggested
466 the decomposition of high-MW (low volatility) species into low-MW (high volatility)
467 compounds. Previous work has also shown fragmentation can play a dominant role in a late stage
468 of heterogeneous oxidation (Kroll et al., 2011). The overall increased volatility may lead to
469 evaporation of smaller redox-active molecules and decrease the DTTt compared to the N_2
470 exposure group. It should also be noted that the O_3 concentrations to which NSOA are exposed
471 here are about 100 times higher than typical ambient levels (Finlayson-Pitts and Pitts Jr, 1999).
472 Assuming heterogeneous oxidation mechanisms are linear and an ambient O_3 concentration of 30
473 ppb, O_3 exposure for 1h, 12h, and 24h under our experimental conditions represent 4, 50, 100
474 days of aging in the atmosphere. Therefore, we anticipate an overall enhancement in OP under
475 ambient conditions. Though similar observations have been made in soot (Antiñolo et al., 2015)
476 and diesel exhausted particles (McWhinney et al., 2013), this enhancement in OP by
477 heterogeneous oxidation is shown here for the first time in SOA particles.
478
479 **3.5 OP changes upon mixing with Cu**
480 Ambient PM forming from mixed sources is frequently composed of both organics and metals.
481 To date, both organics (quinone) and transition metals (Cu, Fe, Mn etc.) have been shown to be

redox-active (Charrier and Anastasio, 2012; Xiong et al., 2017). Metals in ambient particles can range from insoluble substances to soluble cations, leading to various health outcomes after deposition onto the human respiratory tract (Gojova et al., 2007; Oberdörster et al., 2005).

Based on the chemical composition and the assumption that DTT activities of quinones and transition metals are additive, previous studies have attempted to reconstruct the overall OP in ambient particles based on the chemical composition (Charrier and Anastasio, 2012;Charrier et al., 2015). However, addition of a transition-metal chelator did not result in significant changes in the expression of inflammatory biomarkers (Donaldson et al., 2001), suggesting that oxidative activities from different transition metals may not be additive. In our study, significant reductions in OP were observed for PSOA (43±4%) and NSOA (50±6%), when they were mixed with Cu (II) (Fig.8a). Conversely, no significant OP reduction was observed when α-pinene or limonene SOA was mixed with Cu (II). To further investigate the cause of this reduction, we examined the OP of 1,2-NQN, 1,4-NQN, 1,3-DHN and 2,3-DHN and the effects from mixing with Cu(II). Significant OP reductions for 1,2-NQN (42±7%) and 2,3-DHN (35±1%)(Fig. 8b) were observed, but no such changes were observed with 1,4-NQN or 1,3-DHN upon metal mixing. It should be noted that a mixture of phenanthrenequinone and Cu(II) did not show a significant reduction in DTT activity in a study by Charrier and Anastasio (2012) while it is likely that the DTT measurements may be affected by the inefficiency of the quench regent, trichloroacetic acid (Curbo et al., 2013). Furthermore, an increased level of OP reduction was observed when an increasing amount of Cu (II) were mixed with the same amount of 1,2-NQN (Fig. S6). Based on the observation that OP reduction occurs only when there are neighboring oxygenated functional groups, we hypothesize that the OP reduction is related to formation of

505 covalent bonds between the electron-deficient Cu (II) and the electron-donating polar functional
506 groups. The formation of quinone-copper complexes have been demonstrated previously
507 (Dooley et al., 1990; Klinman, 1996), and may be responsible for reducing the overall OP.
508
509 To understand the underlying mechanism, ^{1}H NMR spectroscopy was used to monitor the
510 formation of the organic-Cu complex. ^{1}H NMR has previously been applied to study the binding
511 between metals and organics (Peana et al., 2015; Syme and Viles, 2006). The relaxometry (T2)
512 of NSOA illustrated in Fig. 9 shows a decreasing trend on average for T2 relaxation time when
513 Cu (II) was added to the system. Such decrease in relaxation time indicates interactions between
514 copper and SOA components. Due to the complexity in the SOA NMR spectra, it is still
515 currently challenging to specifically identify binding between individual NSOA components and
516 Cu. To further investigate the binding reactions, ^{1}H NMR measurements were made for the
517 compounds present in NSOA, as previously mentioned, in the presence and absence of Cu, as
518 shown in Fig. 10. Significant interactions between Cu and 1,2-NQN are evidenced by the
519 broadened peak shapes (Fig. 10a), caused by the coordination of adjacent oxygen groups with
520 the copper ion, which has also been well documented in previous studies with similar
521 compounds (Inoue and Gokel, 1990;Schmidt et al., 1990;Tolman, 1977). Protons proximal to the
522 binding sites are more significantly broadened, while protons further away are less affected.
523 Conversely, mixing of 1, 4-NQN with Cu led to little changes in peak shape, indicating the lack
524 of any interactions with copper, as shown in Fig. 10b. Similar phenomena were also observed
525 with another pair of isomers (2, 3-DHN and 1,3-DHN). As shown in Fig.10c, 2, 3-DHN shows a
526 clear change in peak shape indicating that these hydroxyl moieties on adjacent carbons are very

527 important for copper coordination. On the other hand, the 1, 3-DHN structure shows very little
528 peak broadening when mixed with copper.
529
530 Such binding evidence was further supported by NMR relaxation data (Fig. 11). As copper is
531 paramagnetic, it is an effective relaxation agent, and protons brought into its proximity undergo
532 faster T1 and T2 relaxation that manifest themselves as spectral broadening in 1D NMR (Fig. 10).
533 For the epitope maps, the largest circles indicate the least interactions with copper. For both T1
534 and T2 data (Fig. 11, Table S1), protons adjacent to the binding sites a and f (pronto peak
535 assignment based on Fig.10a, Fig.S5) underwent significant changes in relaxation indicating the
536 metal coordinating to the neighboring oxygen groups. Proton e changed less as it is located
537 further away from the copper binding site. While copper has a relatively mild effect on protons b
538 and d, a significant reduction in T1 and T2 for proton c was observed. Such interesting
539 phenomenon is due to the increased nuclear Overhauser effect (NOE) from the b and d sites. In
540 the absence of binding, protons b and d would in part relax via NOE with protons a and e, which
541 relax rapidly due to the copper binding. As such protons b and d can no longer lose
542 magnetization via an Overhauser effect owing to a and e. Instead, they pass magnetization to
543 position c which underwent enhanced level of relaxation as a result. The NOE effect for ring
544 systems with similar structure has also been demonstrated by several previous publications
545 (Kowalewski and Maler, 2006; Rehmann and Barton, 1990). It should be noted that the increased
546 level of OP depletion is accompanied by an increased ratio of Cu to 1,2-NQN (Fig. S4a), the
547 degree of broadening in the 1D NMR proton peaks becomes more significant (Fig. S4b), and the
548 relaxation times T1, T2 decreases (Fig. 11). All these observations together illustrate that the
549 reduction of OP is proportional to the binding between Cu and organics, and further supports the

mechanism behind OP depletion in the DTT assay. Based on the conclusions from the individual organic standards, the overall decrease in relaxation times for NSOA mixing with Cu (shown in Fig. 9) likely indicates that Cu(II) are binding with NSOA components, limiting the redox activities and OP of both the Cu(II) ions and the redox-active NSOA components.

4 Implications

Oxidative stress caused by ROS production and antioxidant consumption is one of the most commonly studied mechanisms for PM toxicity (Nel, 2005;Rhee, 2006;Manke et al., 2013). Here we performed OP evaluation of two SOA formed from PAHs (naphthalene, phenanthrene) by the DTT assay, and investigated the linkages between SOA OP and chemical composition upon various atmospheric aging processes. SOA derived from ozonolysis of monoterpenes (α-pinene, limonene) have a lower DTTm than that of the two PAHs derived SOA, which could be attributed to the high redox-active quinone-like components. This is also consistent with the previous hypothesis that OP of SOA is highly dependent on the identity of its precursor (Tuet et al., 2017a). To further link SOA OP to its chemical composition, this study also explored the possible impacts from atmospheric aging processes so as to provide mechanistic understanding for ambient observations.

Over the span of atmospheric lifetime, the mass and chemical composition of SOA can be affected by aging processes (Kroll et al., 2009; Lim et al., 2017). The aerosol aging processes that we studied here include oligomerization, heterogeneous oxidation and metal mixing. Apart from quinones that are well known to exhibit high OP in aerosol samples, OP contributions from peroxides in our NSOA system are likely to be insignificant. Rather, oxygenated derivatives

were shown here to contribute greater OP than their precursors in our study of selected organic individuals, and heterogeneous oxidation of NSOA was shown to lead to greater OP as well. Moreover, DTT activities of the monomer-rich and oligomer-rich fractions in NSOA separated by liquid chromatography showed oligomers are OP contributors in SOA. While organic peroxides have been proved to be very labile components with half-lives of minutes at room temperature (Krapf et al., 2016), SOA oligomers are relatively stable and highly oxygenated with their ratio of total organic molecular weight per organic carbon weight (OM:OC) similar to that of atmospheric humic-like substances (HULIS)(Altieri et al., 2008). Consistent with OP contributions from oxygenated components enriched HULIS fraction in ambient PM (Verma et al., 2015b), this study also shows evidence for OP contributors from atmospheric aging products of PAH-derived SOA, indicating major organic PM OP contributors could be less volatile than previously thought, and may more readily remain in the particle phase under atmospheric aging. Nevertheless, future work should focus on improving separation methods, allowing for more precise measurements of OP from SOA oligomeric constituents.

A reduction in OP was observed when mixing NSOA/PSOA with Cu (II), resulting in a non-additive effect. However, no such reduction was observed in α-pinene SOA or limonene SOA. Using ^{1}H NMR spectroscopy, we demonstrate that the reduction in OP is likely caused by binding between Cu (II) and redox active organic compounds. Both the peak broadening in 1D NMR spectra and shorter relaxation times are observed for compounds that exhibited OP reduction (1,2-NQN, 2,3-DHN) upon Cu(II) mixing. Additionally, the greater amount of Cu (II) mixed in, the enhanced OP reduction and the decrease in relaxation times showed up. While it is still challenging to determine which NSOA components are binding with Cu (II), the overall

relaxation time also decreased when NSOA was mixed with Cu(II), indicating binding between Cu(II) and various NSOA components. Based on our work, previously recognized redox-active organic and inorganic components in ambient particles (Charrier and Anastasio, 2012; McWhinney et al., 2011; Monks et al., 1992; Turski and Thiele, 2009) may bind with each other once mixed during atmospheric aging processes (external) or within the physiological environment of the human body (internal). The current study demonstrates that such binding leads to a lower OP, which may be relevant to many health outcomes. In the future, a more detailed understanding of SOA binding with metal components and the effects on the oxidative health outcomes will be essential. It should also be noted that the DTT assay alone may not be entirely representative of physiological ROS variations (Tuet et al., 2017a; Xiong et al., 2017;). More *in vitro* and *in vivo* work should be performed in establishing the relationship between chemical composition and the OP of aerosol.

ASSOCIATED CONTENT

Supporting Information.

AUTHOR INFORMATION

Corresponding Author

* Address: 200 College Street, Toronto, ON, M5S 3E5

Email: arthurwh.chan@utoronto.ca

Phone: +1 (416)-978-2602

Notes

The authors declare no competing financial interest.

ACKNOWLEDGEMENT

This work was supported by Natural Sciences and Engineering Research Council Discovery Grant, Canadian Foundation for Innovation John R Evans Leaders Fund, and the Ontario Early Researcher Award. The authors would like to thank Dr. Jon Abbatt, Dr. Greg Evans and Manpreet Takhar for helpful discussion.

References:

Altieri, K., Seitzinger, S., Carlton, A., Turpin, B., Klein, G., and Marshall, A.: Oligomers formed through in-cloud methylglyoxal reactions: Chemical composition, properties, and mechanisms investigated by ultra-high resolution FT-ICR mass spectrometry, Atmos. Environ., 42, 1476-1490, 2008.

Antiñolo, M., Willis, M. D., Zhou, S., and Abbatt, J. P. D.: Connecting the oxidation of soot to its redox cycling abilities, Nat. Commun., 6, 2015.

Atkinson, R., and Arey, J.: Atmospheric degradation of volatile organic compounds, Chem. Rev., 103, 4605-4638, 2003.

Banerjee, D. K., and Budke, C. C.: Spectrophotometric Determination of Traces of Peroxides in Organic Solvents, Anal. Chem., 36, 792-796, 1964.

Beelen, R., Raaschou-Nielsen, O., Stafoggia, M., Andersen, Z. J., Weinmayr, G., Hoffmann, B., Wolf, K., Samoli, E., Fischer, P., and Nieuwenhuijsen, M.: Effects of long-term exposure to air pollution on natural-cause mortality: an analysis of 22 European cohorts within the multicentre ESCAPE project, Lancet, 383, 785-795, 2014.

643 Bolton, J. L., Trush, M. A., Penning, T. M., Dryhurst, G., and Monks, T. J.: Role of quinones in
644 toxicology, Chem. Res. Toxicol., 13, 135-160, 2000.
645 Brunekreef, B., and Holgate, S. T.: Air pollution and health, The lancet, 360, 1233-1242, 2002.
646 Chan, A. W. H., Kautzman, K. E., Chhabra, P. S., Surratt, J. D., Chan, M. N., Crounse, J. D.,
647 Kürten, A., Wennberg, P. O., Flagan, R. C., and Seinfeld, J. H.: Secondary organic aerosol
648 formation from photooxidation of naphthalene and alkylnaphthalenes: implications for oxidation
649 of intermediate volatility organic compounds (IVOCs), Atmos. Chem. Phys., 9, 3049-3060, 2009.
650 Charrier, J. G., and Anastasio, C.: On dithiothreitol (DTT) as a measure of oxidative potential for
651 ambient particles: evidence for the importance of soluble transition metals, Atmos. Chem. Phys.,
652 12, 11317, 2012.
653 Charrier, J. G., Richards-Henderson, N. K., Bein, K. J., McFall, A. S., Wexler, A. S., and
654 Anastasio, C.: Oxidant production from source-oriented particulate matter–Part 1: Oxidative
655 potential using the dithiothreitol (DTT) assay, Atmos. Chem. Phys., 15, 2327-2340, 2015.
656 Charrier, J. G., McFall, A. S., Vu, K. K., Baroi, J., Olea, C., Hasson, A., and Anastasio, C.: A
657 bias in the “mass-normalized” DTT response–An effect of non-linear concentration-response
658 curves for copper and manganese, Atmos. Environ., 144, 325-334, 2016.
659 Cho, A. K., Di Stefano, E., You, Y., Rodriguez, C. E., Schmitz, D. A., Kumagai, Y., Miguel, A.
660 H., Eiguren-Fernandez, A., Kobayashi, T., and Avol, E.: Determination of four quinones in
661 diesel exhaust particles, SRM 1649a, and atmospheric $PM_{2.5}$ special issue of aerosol science and
662 technology on findings from the fine particulate matter supersites program, Aerosol Sci. Tech.,
663 38, 68-81, 2004.

664 Cho, A. K., Sioutas, C., Miguel, A. H., Kumagai, Y., Schmitz, D. A., Singh, M., Eiguren-
665 Fernandez, A., and Froines, J. R.: Redox activity of airborne particulate matter at different sites
666 in the Los Angeles Basin, Environ. Res., 99, 40-47, 2005.
667 Cleland, W. W. : Dithiothreitol, a new protective reagent for SH groups. Biochem., 3(4), 480-
668 482, 1964.
669 Cohen, A. J., Brauer, M., Burnett, R., Anderson, H. R., Frostad, J., Estep, K., Balakrishnan, K.,
670 Brunekreef, B., Dandona, L., and Dandona, R.: Estimates and 25-year trends of the global
671 burden of disease attributable to ambient air pollution: an analysis of data from the Global
672 Burden of Diseases Study 2015, Lancet, 389, 1907-1918, 2017.
673 Curbo, S., Reiser, K., Rundlöf, A. K., Karlsson, A., & Lundberg, M. :Is trichloroacetic acid an
674 insufficient sample quencher of redox reactions? , Antioxid. Redox Sign.,18(7), 795-799, 2013.
675 de Kok, T. M., Driece, H. A., Hogervorst, J. G., and Briedé, J. J.: Toxicological assessment of
676 ambient and traffic-related particulate matter: a review of recent studies, Mutat. Res-Rev. Mutat.,
677 613, 103-122, 2006.
678 Delfino, R. J., Staimer, N., Tjoa, T., Gillen, D. L., Schauer, J. J., and Shafer, M. M.: Airway
679 inflammation and oxidative potential of air pollutant particles in a pediatric asthma panel, J.
680 Expo. Sci. Env. Epid., 23, 466-473, 2013.Di Lorenzo, R. A., and Young, C. J.: Size separation
681 method for absorption characterization in brown carbon: Application to an aged biomass burning
682 sample, Geophys. Res. Lett., 43, 458-465, 2016.
683 Di Lorenzo, R. A., Washenfelder, R. A., Attwood, A. R., Guo, H., Xu, L., Ng, N. L., Weber, R.
684 J., Baumann, K., Edgerton, E., and Young, C. J.: Molecular-Size-Separated Brown Carbon
685 Absorption for Biomass-Burning Aerosol at Multiple Field Sites, Environ. Sci. Technol., 51,
686 3128-3137, 2017.

687 Docherty, K. S., Wu, W., Lim, Y. B., and Ziemann, P. J.: Contributions of organic peroxides to
688 secondary aerosol formed from reactions of monoterpenes with O3, Environ. Sci. Technol., 39,
689 4049-4059, 2005.
690 Donaldson, K., Stone, V., Seaton, A., and MacNee, W.: Ambient particle inhalation and the
691 cardiovascular system: potential mechanisms, Environ. Health Persp., 109, 523, 2001.
692 Dooley, D. M., McIntire, W. S., McGuirl, M. A., Cote, C. E., and Bates, J. L.: Characterization
693 of the active site of Arthrobacter P1 methylamine oxidase: evidence for copper-quinone
694 interactions, J. Am. Chem. Soc., 112, 2782-2789, 10.1021/ja00163a047, 1990.
695 Fang, T., Guo, H., Verma, V., Peltier, R. E., and Weber, R. J.: PM 2.5 water-soluble elements in
696 the southeastern United States: automated analytical method development, spatiotemporal
697 distributions, source apportionment, and implications for heath studies, Atmos. Chem. Phys., 15,
698 11667-11682, 2015.
699 Fang, T., Verma, V., Bates, J. T., Abrams, J., Klein, M., Strickland, M. J., Sarnat, S. E., Chang,
700 H. H., Mulholland, J. A., and Tolbert, P. E.: Oxidative potential of ambient water-soluble PM 2.5
701 in the southeastern United States: contrasts in sources and health associations between ascorbic
702 acid (AA) and dithiothreitol (DTT) assays, Atmos. Chem. Phys., 16, 3865-3879, 2016.
703 Finlayson-Pitts, B. J., and Pitts Jr, J. N.: Chemistry of the upper and lower atmosphere: theory,
704 experiments, and applications, Academic press, 1999.
705 Gao, S., Ng, N. L., Keywood, M., Varutbangkul, V., Bahreini, R., Nenes, A., He, J., Yoo, K. Y.,
706 Beauchamp, J. L., and Hodyss, R. P.: Particle phase acidity and oligomer formation in secondary
707 organic aerosol, Environ. Sci. Technol., 38, 6582-6589, 2004.
708 George, I., and Abbatt, J.: Heterogeneous oxidation of atmospheric aerosol particles by gas-
709 phase radicals, Nat. Chem., 2, 713-722, 2010.

710 Godri, K. J., Harrison, R. M., Evans, T., Baker, T., Dunster, C., Mudway, I. S., and Kelly, F. J.:
711 Increased oxidative burden associated with traffic component of ambient particulate matter at
712 roadside and urban background schools sites in London, PloS one, 6, e21961, 2011.
713 Gojova, A., Guo, B., Kota, R. S., Rutledge, J. C., Kennedy, I. M., and Barakat, A. I.: Induction
714 of inflammation in vascular endothelial cells by metal oxide nanoparticles: effect of particle
715 composition, Environ. Health Persp., 403-409, 2007.
716 Groessl, M., Graf, S., and Knochenmuss, R.: High resolution ion mobility-mass spectrometry for
717 separation and identification of isomeric lipids, Analyst, 140, 6904-6911, 2015.
718 Hallquist, M., Wenger, J., Baltensperger, U., Rudich, Y., Simpson, D., Claeys, M., Dommen, J.,
719 Donahue, N., George, C., and Goldstein, A.: The formation, properties and impact of secondary
720 organic aerosol: current and emerging issues, Atmos. Chem. Phys., 9, 5155-5236, 2009.
721 Hansen, R. E., Roth, D., and Winther, J. R. : Quantifying the global cellular thiol–disulfide status.
722 P. Natl. Acad. Sci., 106(2), 422-427, 2009.
723 Inoue, Y., and Gokel, W.G.: Cation Binding by Macrocycles. Complexation of cationic species
724 by crown ethers, Marcel Dekker, New York, 1990.
725 Jiang, H., Jang, M., and Yu, Z.: Dithiothreitol Activity by Particulate Oxidizers of SOA
726 Produced from Photooxidation of Hydrocarbons under Varied NOx Levels, Atmos. Chem. Phys.
727 Discuss., 2017, 1-24, doi:10.5194/acp-2017-214, 2017.
728 Jimenez, J. L., Canagaratna, M. R., Donahue, N. M., Prevot, A. S. H., Zhang, Q., Kroll, J. H.,
729 DeCarlo, P. F., Allan, J. D., Coe, H., and Ng, N. L.: Evolution of organic aerosols in the
730 atmosphere, Science, 326, 1525-1529, 2009.

731 Jokinen, T., Sipilä, M., Richters, S., Kerminen, V. M., Paasonen, P., Stratmann, F., Worsnop, D.,
732 Kulmala, M., Ehn, M., and Herrmann, H.: Rapid autoxidation forms highly oxidized RO2
733 radicals in the atmosphere, Angew. Chem. Int. Edit., 53, 14596-14600, 2014.
734 Kalberer, M., Paulsen, D., Sax, M., Steinbacher, M., Dommen, J., Prevot, A., Fisseha, R.,
735 Weingartner, E., Frankevich, V., and Zenobi, R.: Identification of polymers as major components
736 of atmospheric organic aerosols, Science, 303, 1659-1662, 2004.
737 Kautzman, K. E., Surratt, J. D., Chan, M. N., Chan, A. W. H., Hersey, S. P., Chhabra, P. S.,
738 Dalleska, N. F., Wennberg, P. O., Flagan, R. C., and Seinfeld, J. H.: Chemical composition of
739 gas-and aerosol-phase products from the photooxidation of naphthalene, J. Phys. Chem. A, 114,
740 913-934, 2009.
741 Keywood, M. D., Kroll, J. H., Varutbangkul, V., Bahreini, R., Flagan, R. C., and Seinfeld, J. H.:
742 Secondary organic aerosol formation from cyclohexene ozonolysis: Effect of OH scavenger and
743 the role of radical chemistry, Environ. Sci. Technol., 38, 3343-3350, 2004.
744 Klinman, J. P.: Mechanisms whereby mononuclear copper proteins functionalize organic
745 substrates, Chem. Rev., 96, 2541-2562, 1996.
746 Kostenidou, E., Pathak, R. K., and Pandis, S. N.: An algorithm for the calculation of secondary
747 organic aerosol density combining AMS and SMPS data, Aerosol Sci. Technol., 41, 1002-1010,
748 2007.
749 Kowalewski, J., and Maler, L.: Nuclear spin relaxation in liquids: theory, experiments, and
750 applications, CRC press, 2006.
751 Kramer, A. J., Rattanavaraha, W., Zhang, Z., Gold, A., Surratt, J. D., and Lin, Y.-H.: Assessing
752 the oxidative potential of isoprene-derived epoxides and secondary organic aerosol, Atmos.
753 Environ., 130, 211-218, 2016.

754 Krapf, M., El Haddad, I., Bruns, Emily A., Molteni, U., Daellenbach, Kaspar R., Prévôt, André S.
755 H., Baltensperger, U., and Dommen, J.: Labile Peroxides in Secondary Organic Aerosol, Chem,
756 1, 603-616, 2016.
757 Krapf, M., Künzi, L., Allenbach, S., Bruns, E. A., Gavarini, I., El-Haddad, I., Slowik, J. G.,
758 Prévôt, A. S. H., Drinovec, L., and Močnik, G.: Wood combustion particles induce adverse
759 effects to normal and diseased airway epithelia, Environ. Sci. Proc. Impacts, 2017.
760 Krechmer, J. E., Lambe, A. T., Kimmel, J. R., Cubison, M. J., Budisulistiorini, S. H., Surratt, J.
761 D., Jayne, J. T., Worsnop, D. R., and Canagaratna, M. R.: Ion mobility spectrometry-mass
762 spectrometry (IMS-MS) for on-and offline analysis of atmospheric gas and aerosol species,
763 Atmos. Meas. Tech., 9, 3245, 2016.
764 Kroll, J. H., Smith, J. D., Che, D. L., Kessler, S. H., Worsnop, D. R., and Wilson, K. R.:
765 Measurement of fragmentation and functionalization pathways in the heterogeneous oxidation of
766 oxidized organic aerosol, Phys. Chem. Chem. Phys., 11, 8005-8014, 2009.
767 Kroll, J. H., Donahue, N. M., Jimenez, J. L., Kessler, S. H., Canagaratna, M. R., Wilson, K. R.,
768 Altieri, K. E., Mazzoleni, L. R., Wozniak, A. S., and Bluhm, H.: Carbon oxidation state as a
769 metric for describing the chemistry of atmospheric organic aerosol, Nat. Chem., 3, 133-139,
770 2011.
771 Kumagai, Y., Koide, S., Taguchi, K., Endo, A., Nakai, Y., Yoshikawa, T., and Shimojo, N.:
772 Oxidation of proximal protein sulfhydryls by phenanthraquinone, a component of diesel exhaust
773 particles, Chem. Res. Toxicol., 15, 483-489, 2002.
774 Lee, J. Y., and Lane, D. A.: Unique products from the reaction of naphthalene with the hydroxyl
775 radical, Atmos. Environ., 43, 4886-4893, 2009.

776 Lelieveld, J., Evans, J. S., Fnais, M., Giannadaki, D., and Pozzer, A.: The contribution of outdoor
777 air pollution sources to premature mortality on a global scale, Nature, 525, 367-371, 2015.
778 Li, N., Hao, M., Phalen, R. F., Hinds, W. C., and Nel, A. E.: Particulate air pollutants and asthma:
779 a paradigm for the role of oxidative stress in PM-induced adverse health effects, Clin. Immunol.,
780 109, 250-265, 2003a.
781 Li, N., Sioutas, C., Cho, A., Schmitz, D., Misra, C., Sempf, J., Wang, M., Oberley, T., Froines, J.,
782 and Nel, A.: Ultrafine particulate pollutants induce oxidative stress and mitochondrial damage,
783 Environ. Health Persp., 111, 455, 2003b.
784 Lim, C. Y., Browne, E. C., Sugrue, R. A., and Kroll, J. H. : Rapid heterogeneous oxidation of
785 organic coatings on submicron aerosols. Geophys. Res. Lett., 44(6), 2949-2957,2017.
786 Lin, Y., Arashiro, M., Martin, E., Chen, Y., Zhang, Z., Sexton, K. G., Gold, A., Jaspers, I., Fry,
787 R. C., and Surratt, J. D.: Isoprene-Derived Secondary Organic Aerosol Induces the Expression of
788 Oxidative Stress Response Genes in Human Lung Cells, Environ. Sci. Technol. L., 3, 250-254,
789 2016.
790 Manke, A., Wang, L., and Rojanasakul, Y.: Mechanisms of nanoparticle-induced oxidative stress
791 and toxicity, Biomed. Res. Int., 2013, 1-15, 2013.
792 McWhinney, R. D., Gao, S. S., Zhou, S., and Abbatt, J. P. D.: Evaluation of the effects of ozone
793 oxidation on redox-cycling activity of two-stroke engine exhaust particles, Environ. Sci.
794 Technol., 45, 2131-2136, 2011.
795 McWhinney, R. D., Zhou, S., and Abbatt, J. P. D.: Naphthalene SOA: redox activity and
796 naphthoquinone gas–particle partitioning, Atmos. Chem. Phys., 13, 9731-9744, 2013.
797 Monks, T. J., Hanzlik, R. P., Cohen, G. M., Ross, D., and Graham, D. G.: Quinone chemistry
798 and toxicity, Toxicol. Appl. Pharm., 112, 2-16, 1992.

799 Nel, A.: Air pollution-related illness: effects of particles, Science, 308, 804-806, 2005.

800 Nel, A. E., Diaz-Sanchez, D., Ng, D., Hiura, T., and Saxon, A.: Enhancement of allergic
801 inflammation by the interaction between diesel exhaust particles and the immune system, J.
802 Allergy. Clin. Immun., 102, 539-554, 1998.

803 Oberdörster, G., Oberdörster, E., and Oberdörster, J.: Nanotoxicology: an emerging discipline
804 evolving from studies of ultrafine particles, Environ. Health Persp., 823-839, 2005.

805 Peana, M., Medici, S., Nurchi, V. M., Lachowicz, J. I., Crisponi, G., Crespo-Alonso, M., Santos,
806 M. A., and Zoroddu, M. A.: An NMR study on the 6,6′-(2-
807 (diethylamino)ethylazanediyl)bis(methylene)bis(5-hydroxy-2-hydroxymethyl-4H-pyran-4-one)
808 interaction with AlIII and ZnII ions, J. Inorg. Biochem., 148, 69-77,
809 https://doi.org/10.1016/j.jinorgbio.2015.01.016, 2015.

810 Pope, C. A., Burnett, R. T., Thun, M. J., Calle, E. E., Krewski, D., Ito, K., and Thurston, G. D.:
811 Lung cancer, cardiopulmonary mortality, and long-term exposure to fine particulate air pollution,
812 Jama, 287, 1132-1141, 2002.

813 Pope, C. A., Ezzati, M., and Dockery, D. W.: Fine-particulate air pollution and life expectancy in
814 the United States, N. Engl. J. Med., 2009, 376-386, 2009.

815 Pöschl, U., and Shiraiwa, M.: Multiphase chemistry at the atmosphere–biosphere interface
816 influencing climate and public health in the anthropocene, Chem. Rev., 115, 4440-4475, 2015.

817 Rehmann, J. P., and Barton, J. K.: Proton NMR studies of tris (phenanthroline) metal complexes
818 bound to oligonucleotides: characterization of binding modes, Biochem., 29, 1701-1709, 1990.

819 Rhee, S. G.: H_2O_2, a necessary evil for cell signaling, Science, 312, 1882-1883, 2006.

820 Risom, L., Møller, P., and Loft, S.: Oxidative stress-induced DNA damage by particulate air
821 pollution, Mutat.Res-Fund. Mol. M., 592, 119-137, 2005.

822 Rudich, Y., Donahue, N. M., and Mentel, T. F.: Aging of organic aerosol: Bridging the gap
823 between laboratory and field studies, Annu. Rev. Phys. Chem., 58, 321-352, 2007.
824 Schmidt, M. H., Miskelly, G. M., and Lewis, N. S.: Effects of redox potential, steric
825 configuration, solvent, and alkali metal cations on the binding of carbon dioxide to cobalt (I) and
826 nickel (I) macrocycles, J. Am. Chem. Soc., 112, 3420-3426, 1990.
827 Shen, H., Barakat, A. I., and Anastasio, C.: Generation of hydrogen peroxide from San Joaquin
828 Valley particles in a cell-free solution, Atmos. Chem. Phys., 11, 753-765, 2011.
829 Shilling, J. E., Chen, Q., King, S. M., Rosenoern, T., Kroll, J. H., Worsnop, D. R., DeCarlo, P. F.,
830 Aiken, A. C., Sueper, D., and Jimenez, J. L.: Loading-dependent elemental composition of α-
831 pinene SOA particles, Atmos. Chem. Phys., 9, 771-782, 2009.
832 Shiraiwa, M., Selzle, K., and Pöschl, U.: Hazardous components and health effects of
833 atmospheric aerosol particles: reactive oxygen species, soot, polycyclic aromatic compounds and
834 allergenic proteins, Free. Radical. Res., 46, 927-939, 2012.
835 Simpson, A. J., McNally, D. J., and Simpson, M. J.: NMR spectroscopy in environmental
836 research: from molecular interactions to global processes, Prog. Nucl. Mag. Res. Sp., 58, 97-175,
837 2011.
838 Simpson, M. J., and Simpson, A. J.: NMR Spectroscopy: A Versatile Tool for Environmental
839 Research, John Wiley & Sons, 2014.
840 Smith, M. E., and van Eck, E. R.: Recent advances in experimental solid state NMR
841 methodology for half-integer spin quadrupolar nuclei, Prog. Nucl. Mag. Res. Sp., 34, 159-201,
842 1999.
843 Surratt, J. D., Chan, A. W. H., Eddingsaas, N. C., Chan, M., Loza, C. L., Kwan, A. J., Hersey, S.
844 P., Flagan, R. C., Wennberg, P. O., and Seinfeld, J. H.: Reactive intermediates revealed in

845 secondary organic aerosol formation from isoprene, P. Natl. Acad. Sci., 107, 6640-6645,
846 10.1073/pnas.0911114107, 2010.
847 Syme, C. D., and Viles, J. H.: Solution 1 H NMR investigation of Zn 2+ and Cd 2+ binding to
848 amyloid-beta peptide (Aβ) of Alzheimer's disease, BBA-Proteins and Proteom., 1764, 246-256,
849 2006.
850 Thurston, G. D., Burnett, R. T., Turner, M. C., Shi, Y., Krewski, D., Lall, R., Ito, K., Jerrett, M.,
851 Gapstur, S. M., and Diver, W. R.: Ischemic heart disease mortality and long-term exposure to
852 source-related components of US fine particle air pollution, Environ. Health Persp., 124, 785,
853 2016.
854 Tolman, C. A.: Steric effects of phosphorus ligands in organometallic chemistry and
855 homogeneous catalysis, Chem. Rev., 77, 313-348, 1977.
856 Tolocka, M. P., Jang, M., Ginter, J. M., Cox, F. J., Kamens, R. M., and Johnston, M. V.:
857 Formation of oligomers in secondary organic aerosol, Environ. Sci. Technol., 38, 1428-1434,
858 2004.
859 Trump, E. R., and Donahue, N. M.: Oligomer formation within secondary organic aerosols:
860 equilibrium and dynamic considerations, Atmos. Chem. Phys., 14, 3691-3701, 2014.
861 Tuet, W. Y., Fok, S., Verma, V., Rodriguez, M. S. T., Grosberg, A., Champion, J. A., and Ng, N.
862 L.: Dose-dependent intracellular reactive oxygen and nitrogen species (ROS/RNS) production
863 from particulate matter exposure: comparison to oxidative potential and chemical composition,
864 Atmos. Environ., 144, 335-344, 2016.
865 Tuet, W. Y., Chen, Y., Fok, S., Champion, J. A., and Ng, N. L.: Inflammatory responses to
866 secondary organic aerosols (SOA) generated from biogenic and anthropogenic precursors,
867 Atmos. Chem. Phys. Discuss., 2017, 1-42, 10.5194/acp-2017-262, 2017a.

868 Tuet, W. Y., Chen, Y., Xu, L., Fok, S., Gao, D., Weber, R. J., and Ng, N. L.: Chemical oxidative
869 potential of secondary organic aerosol (SOA) generated from the photooxidation of biogenic and
870 anthropogenic volatile organic compounds, Atmos. Chem. Phys., 17, 839-853, 2017b.
871 Turski, M. L., and Thiele, D. J.: New roles for copper metabolism in cell proliferation, signaling,
872 and disease, J. Biol. Chem., 284, 717-721, 2009.
873 Valavanidis, A., Fiotakis, K., Bakeas, E., and Vlahogianni, T.: Electron paramagnetic resonance
874 study of the generation of reactive oxygen species catalysed by transition metals and quinoid
875 redox cycling by inhalable ambient particulate matter, Redox. Rep., 10, 37-51, 2005.
876 Verma, V., Ning, Z., Cho, A. K., Schauer, J. J., Shafer, M. M., and Sioutas, C.: Redox activity of
877 urban quasi-ultrafine particles from primary and secondary sources, Atmos. Environ., 43, 6360-
878 6368, 2009.
879 Verma, V., Fang, T., Xu, L., Peltier, R. E., Russell, A. G., Ng, N. L., and Weber, R. J.: Organic
880 aerosols associated with the generation of reactive oxygen species (ROS) by water-soluble $PM_{2.5}$,
881 Environ. Sci. Technol., 49, 4646-4656, 2015a.
882 Verma, V., Wang, Y., El-Afifi, R., Fang, T., Rowland, J., Russell, A. G., and Weber, R. J.:
883 Fractionating ambient humic-like substances (HULIS) for their reactive oxygen species activity–
884 Assessing the importance of quinones and atmospheric aging, Atmos. Environ., 120, 351-359,
885 2015b.
886 Wang, L., Xu, W., Khalizov, A. F., Zheng, J., Qiu, C., and Zhang, R.: Laboratory investigation
887 on the role of organics in atmospheric nanoparticle growth, J. Phys. Chem. A, 115, 8940-8947,
888 2011.

889 Xiong, Q., Yu, H., Wang, R., Wei, J., and Verma, V.: Rethinking The Dithiothreitol (DTT)
890 Based PM Oxidative Potential: Measuring DTT Consumption versus ROS Generation, Environ.
891 Sci. Technol., 2017.
892 Ye, J., Gordon, C. A., and Chan, A. W. H.: Enhancement in secondary organic aerosol formation
893 in the presence of preexisting organic particle, Environ. Sci. Technol., 50, 3572-3579, 2016.
894 Ye, J., Salehi, S., North, M. L., Portelli, A. M., Chow, C.-W., and Chan, A. W. H.: Development
895 of a Novel Simulation Reactor for Chronic Exposure to Atmospheric Particulate Matter, Sci.
896 Rep., 7, 2017.
897 Zhang, R., Wang, G., Guo, S., Zamora, M. L., Ying, Q., Lin, Y., Wang, W., Hu, M., and Wang,
898 Y.: Formation of urban fine particulate matter, Chem. Rev., 115, 3803-3855, 2015.
899 Zhang, X., McVay, R. C., Huang, D. D., Dalleska, N. F., Aumont, B., Flagan, R. C., and
900 Seinfeld, J. H.: Formation and evolution of molecular products in α-pinene secondary organic
901 aerosol, P. Natl. Acad. Sci., 112, 14168-14173, 2015.
902 Zhang, X., Lambe, A. T., Upshur, M. A., Brooks, W. A., Gray Be, A., Thomson, R. J., Geiger, F.
903 M., Surratt, J. D., Zhang, Z., and Gold, A.: Highly Oxygenated Multifunctional Compounds in α-
904 pinene Secondary Organic Aerosol, Environ. Sci. Technol., 2017.
905
906
907
908
909

Atmos. Chem. Phys. Discuss., https://doi.org/10.5194/acp-2017-1012
Manuscript under review for journal Atmos. Chem. Phys.
Discussion started: 10 November 2017

Atmospheric Chemistry and Physics Discussions

Table 1. Flow tube experimental conditions

Compund	Reaction[a]	ΔHC ppb	Y[b,c] %	RH
limonene	ozonolysis	251±23	25±3.9	14±1%
α-pinene	ozonolysis	304±17	19±4.2	14±1%
naphthalene	photooxidation	6436±402	28±6.7	57 ±5%
phenanthrene	photooxidation	4050±578	12±2.6	57 ±5%

a. Temperature in all experiments is around room temperature (22-25℃).
b. SOA mass yields were calculated without particle wall loss correction.
c. SOA density in this study was assumed to be 1.25 g cm^{-3} for monoterpene SOA (Shilling et al., 2009), and 1.55 g cm^{-3} for PAHs SOA(Chan et al., 2009).

Table 2. SOA peroxide content and OP

Organics	Peroxide percentage %	DTTm pmol min^{-1} μg^{-1}
Naphthalene SOA	<3%	100-129
α-pinene SOA	40-100%	10-20
Benzoyl peroxide	100%	160

Atmos. Chem. Phys. Discuss., https://doi.org/10.5194/acp-2017-1012
Manuscript under review for journal Atmos. Chem. Phys.
Discussion started: 10 November 2017

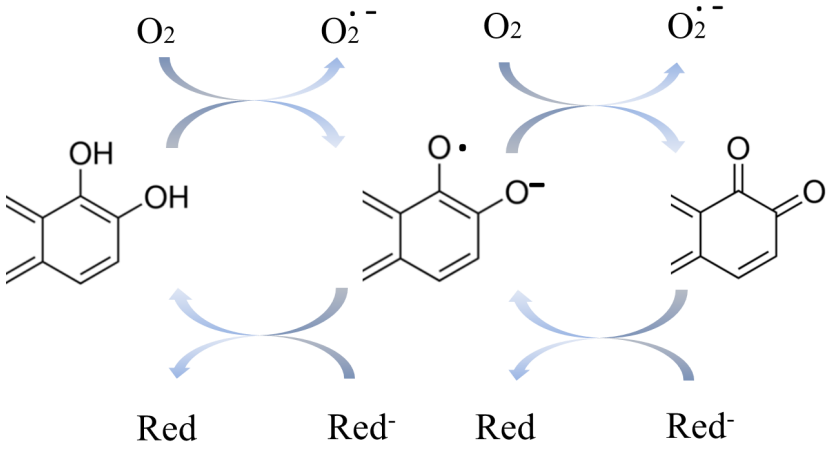

Figure 1. A simplified mechanism of redox cycling of quinone-like substances and formation of superoxide anion radicals. ***Red*** refers to a general reductant. In the redox cycle, regenerated quinone serves as a chemical intermediate to transfer electrons from reductants to oxygen to form superoxide ($O_2^{\cdot -}$).

Atmos. Chem. Phys. Discuss., https://doi.org/10.5194/acp-2017-1012
Manuscript under review for journal Atmos. Chem. Phys.
Discussion started: 10 November 2017

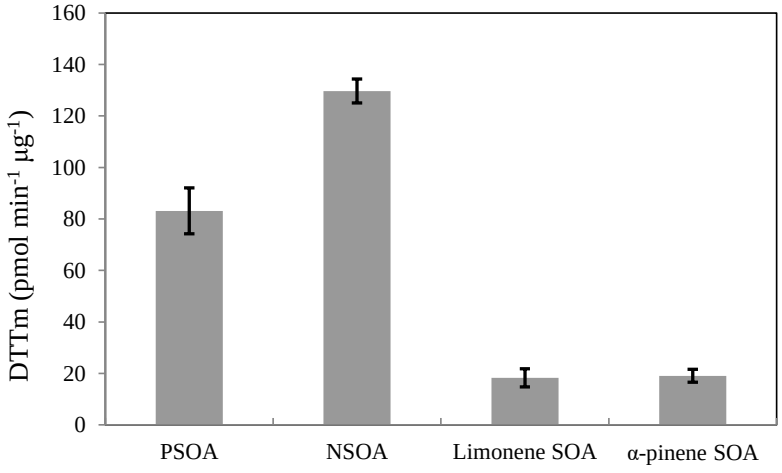

Figure 2. DTTm (pmol min^{-1} μg^{-1}) for SOA formed from various types of hydrocarbons (phenanthrene, naphthalene, limonene and α-pinene). Each measurement was conducted in triplicates, and the error bar represents the standard error of the mean (SEM).

Atmos. Chem. Phys. Discuss., https://doi.org/10.5194/acp-2017-1012
Manuscript under review for journal Atmos. Chem. Phys.
Discussion started: 10 November 2017

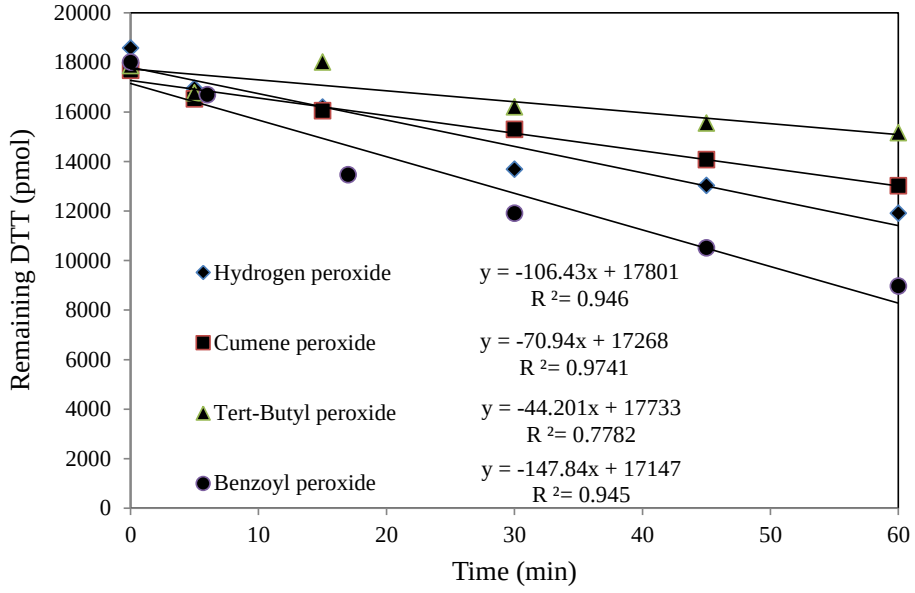

Figure 3. DTT activity of various types of peroxides (hydrogen peroxide, cumene peroxide, tert-Butyl peroxide, benzoyl peroxide). With the same initial concentration of peroxide (0.1mM), benzoyl peroxide has the highest DTT activity (147.8 pmol min^{-1}, which can be converted to DTTm of 38 pmol min^{-1} ug^{-1}).

Atmos. Chem. Phys. Discuss., https://doi.org/10.5194/acp-2017-1012
Manuscript under review for journal Atmos. Chem. Phys.
Discussion started: 10 November 2017

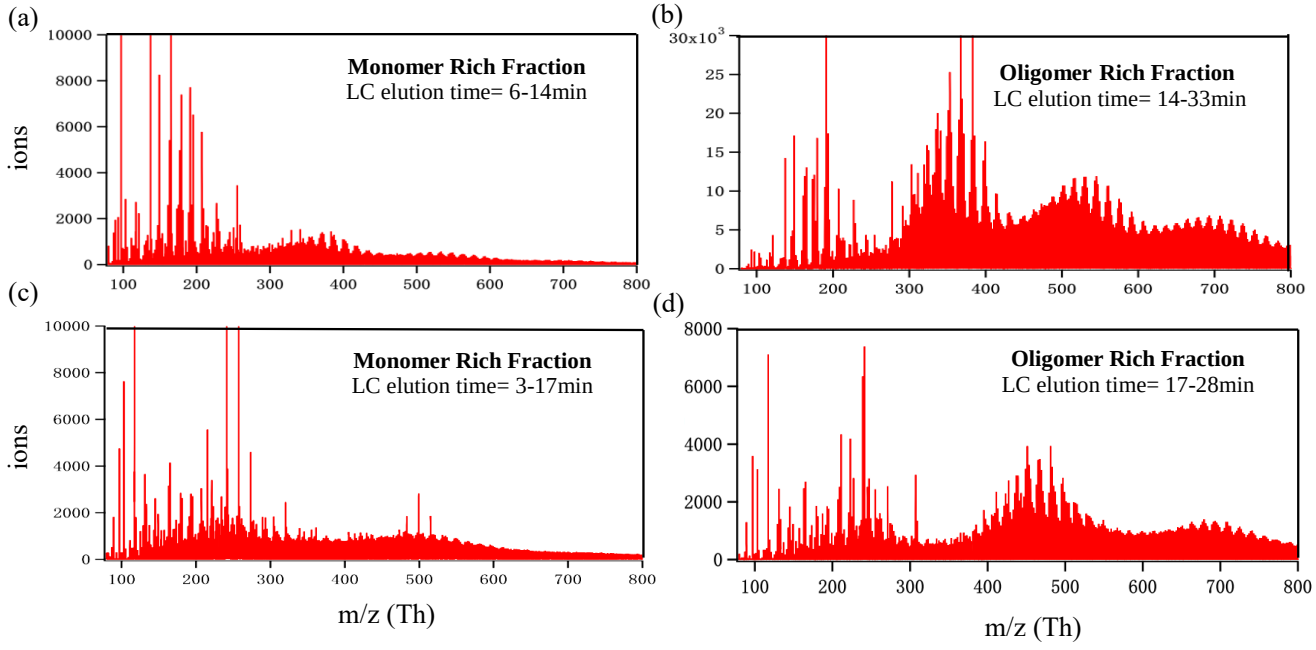

Figure 4. IMS-TOF mass spectra for (a) monomer-rich fraction (b) oligomer-rich fraction in NSOA and (c) monomer-rich fraction (d) oligomer-rich fraction in PSOA. During a total of 46-min elution, the majority of NSOA monomers eluted at 6-14 min, and most of the oligomers eluted at 14-33min. For PSOA system, the majority of monomers eluted at 3-17 min, and most of the oligomer- rich fraction eluted at 17-28 min.

Atmos. Chem. Phys. Discuss., https://doi.org/10.5194/acp-2017-1012
Manuscript under review for journal Atmos. Chem. Phys.
Discussion started: 10 November 2017

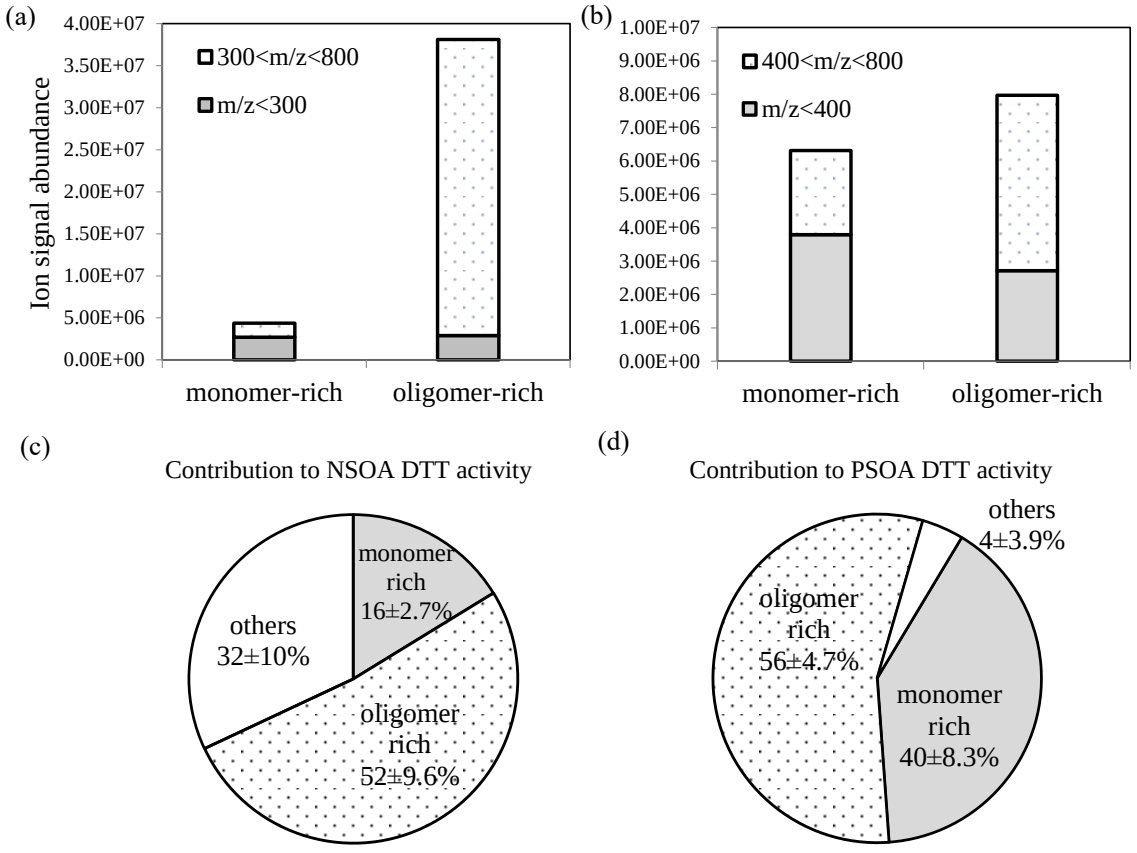

Figure 5. Sum of ion signals for monomers and oligomers in monomer-rich fraction and oligomer-rich fraction for NSOA (a) and PSOA (b) systems. OP (DTTt) contributions from monomer-rich fraction and oligomer-rich fraction in NSOA (c) and PSOA (d) systems. The remaining DTT activity (others, white) is attributed to residual SOA fractions that did not clearly elute out.

Atmos. Chem. Phys. Discuss., https://doi.org/10.5194/acp-2017-1012
Manuscript under review for journal Atmos. Chem. Phys.
Discussion started: 10 November 2017

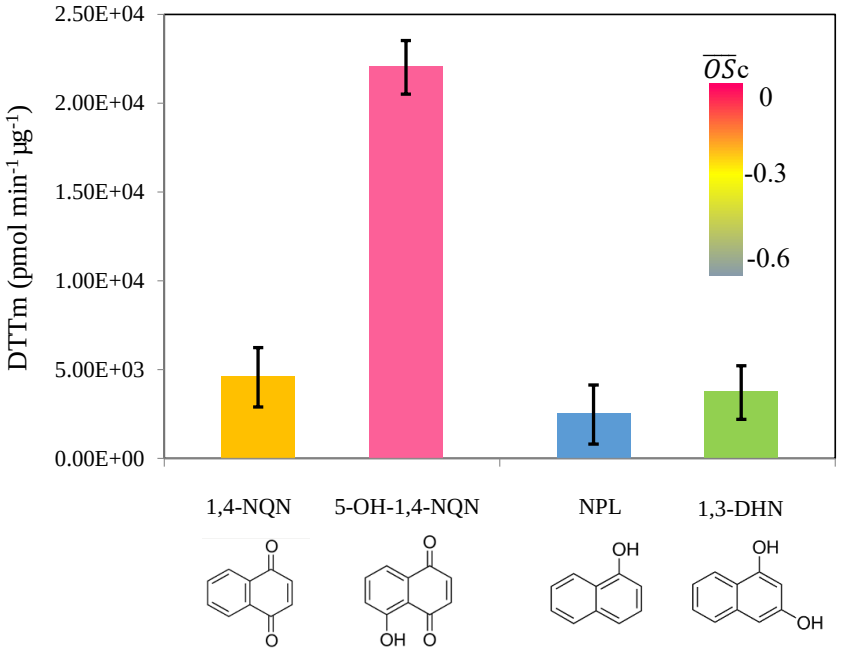

Figure 6. DTTm for two selected pairs of oxygenated derivatives in NSOA system (1,4-NQN vs. 5-OH 1,4-NQN, NPL vs. 1,3-DHN). Averaged carbon oxidation state ($\overline{OS}$c) of each component is shown in color (color scale shown on top-right). Each measurement was conducted in triplicates, and the error bar here represents the SEM. The asterisk indicates significant difference between each pair of measurements at the 95% confidence level.

Atmos. Chem. Phys. Discuss., https://doi.org/10.5194/acp-2017-1012
Manuscript under review for journal Atmos. Chem. Phys.
Discussion started: 10 November 2017

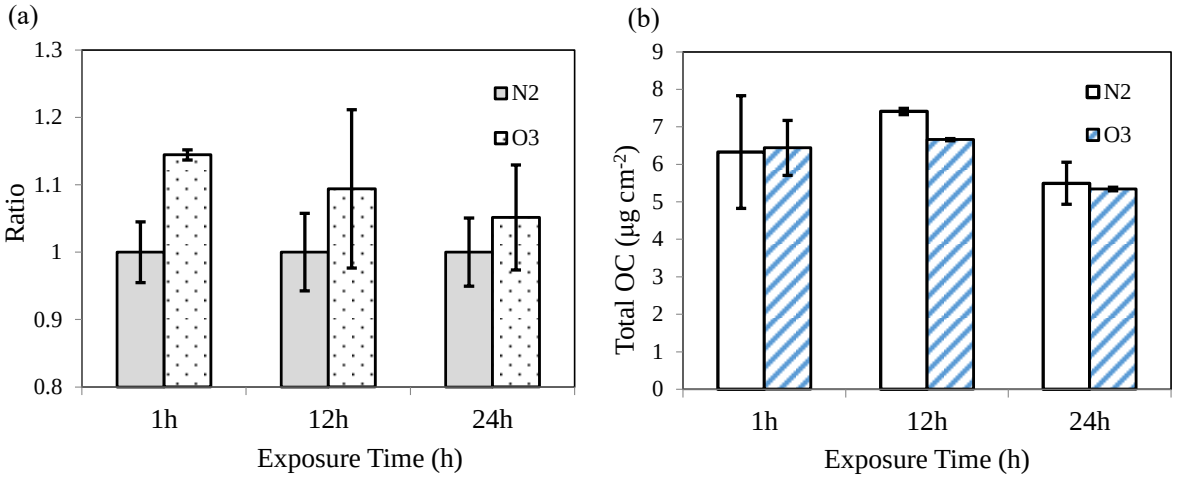

Figure 7. (a) Relative DTTt for NSOA after O_3 and N_2 exposure. For each of the exposure duration (1h, 12h, 24h), the DTTt of O_3 exposure group was normalized by the DTTt of the corresponding N_2 exposure group. Generally, DTTt of NSOA that underwent heterogeneous ozonolysis was higher than that of the N_2 control. (b) OC/EC measurement results show total OC mass loss (17% and 13% for O_3 and N_2 exposure, respectively) after 24-hour exposures. Each measurement was conducted in triplicates, and the error bar represents the SEM.

Atmos. Chem. Phys. Discuss., https://doi.org/10.5194/acp-2017-1012
Manuscript under review for journal Atmos. Chem. Phys.
Discussion started: 10 November 2017

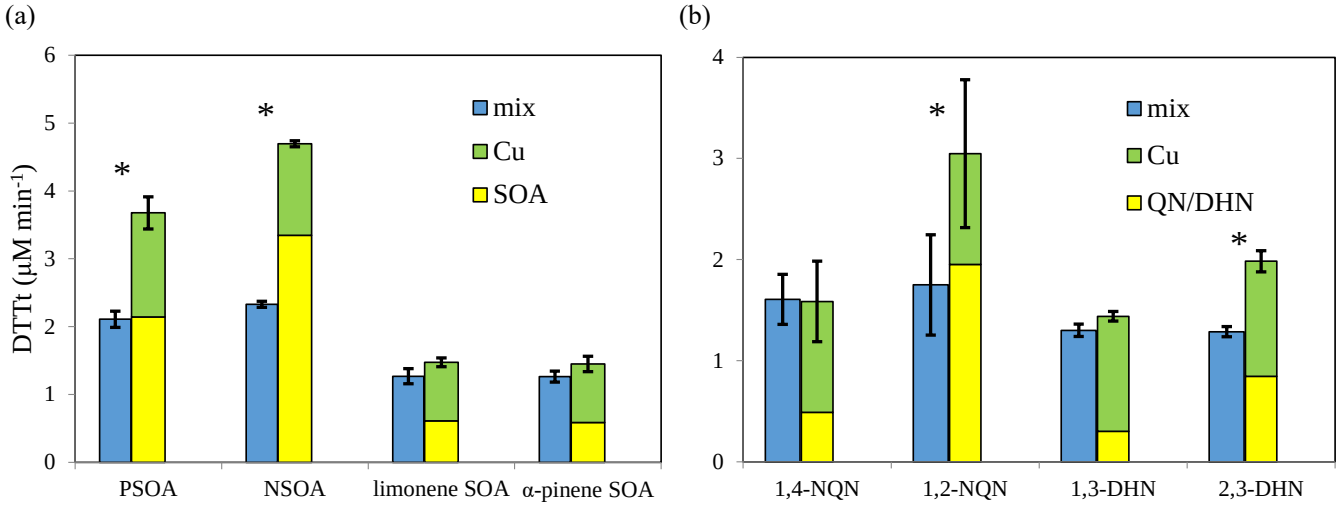

Figure 8. Significant OP depletions were observed when PSOA(43±4%), NSOA(50±6%), 1,2-NQN(42±7%) and 2,3-DHN(35±1%) mixed with Cu (II). The asterisk indicates significant difference between a pair of bars at a 95% confidence level.

Atmos. Chem. Phys. Discuss., https://doi.org/10.5194/acp-2017-1012
Manuscript under review for journal Atmos. Chem. Phys.
Discussion started: 10 November 2017

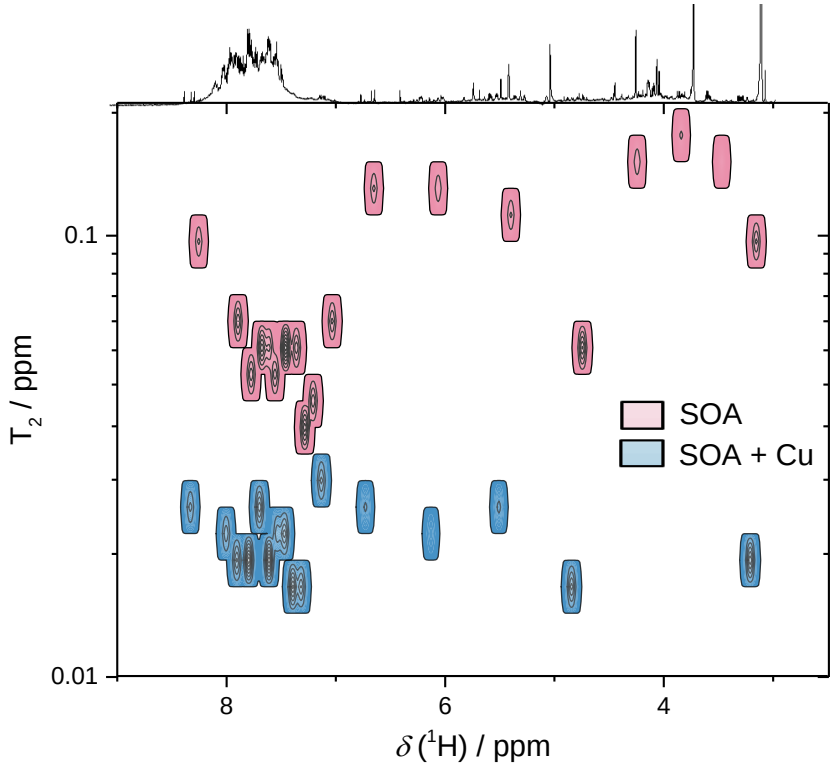

Figure 9. 2D ^{1}H-NMR T2 relaxation contour map for NSOA with (blue) and without copper (red) with 1D NMR projections from the top. A general decreasing trend in T2 is observed here, which indicates interactions (binding) of Cu (II) with many NSOA components.

Atmos. Chem. Phys. Discuss., https://doi.org/10.5194/acp-2017-1012
Manuscript under review for journal Atmos. Chem. Phys.
Discussion started: 10 November 2017

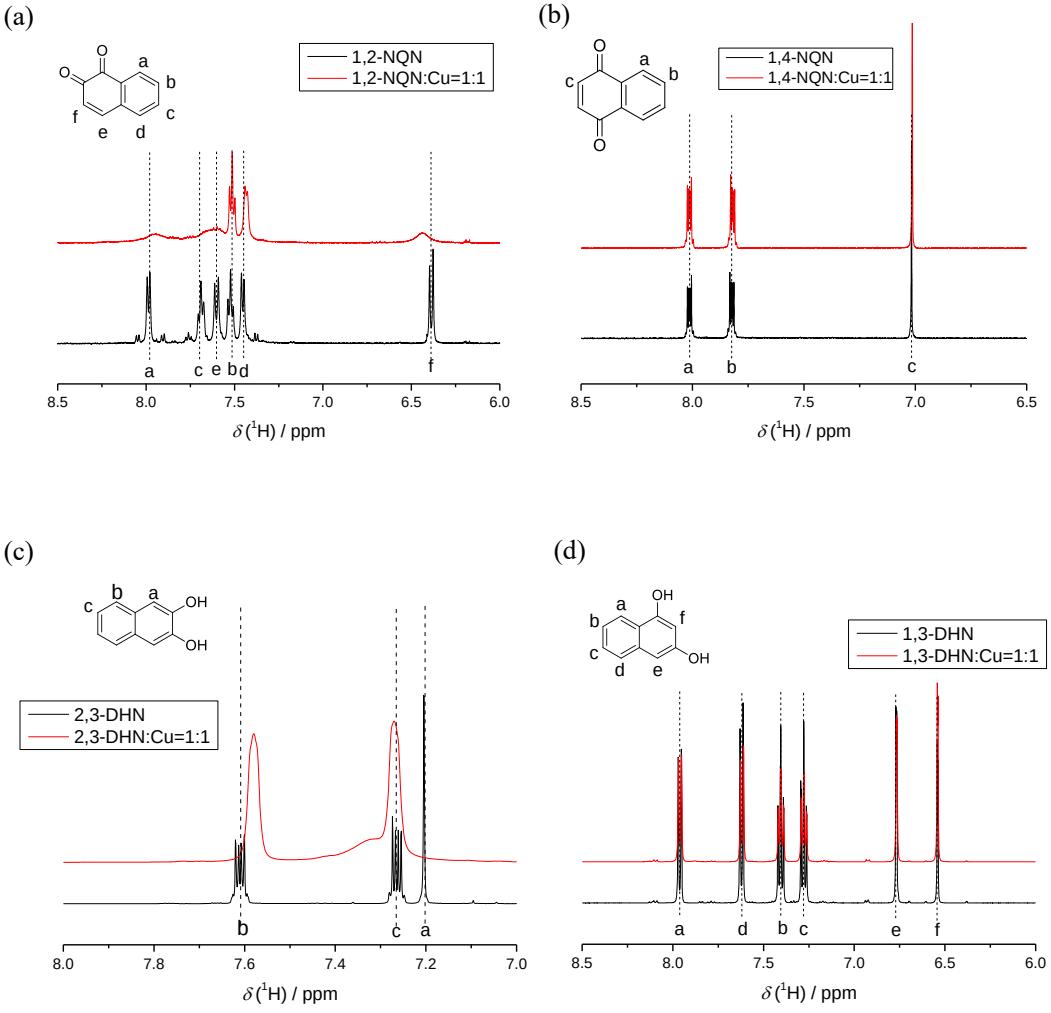

Figure 10. 1 D ^{1}H-NMR spectra of (a) 1,2-NQN (b) 1,4-NQN (c) 2,3-DHN (d)1,3-DHN and their mixture with 1:1 ratio of Cu (II). Both 1,2-NQN and 2,3-DHN show the broadening of ^{1}H-NMR peaks (protons at a, c, e, f and a, b, c for 1,2-NQN and 2,3-DHN, respectively) after mixing with Cu(II).

Atmos. Chem. Phys. Discuss., https://doi.org/10.5194/acp-2017-1012
Manuscript under review for journal Atmos. Chem. Phys.
Discussion started: 10 November 2017

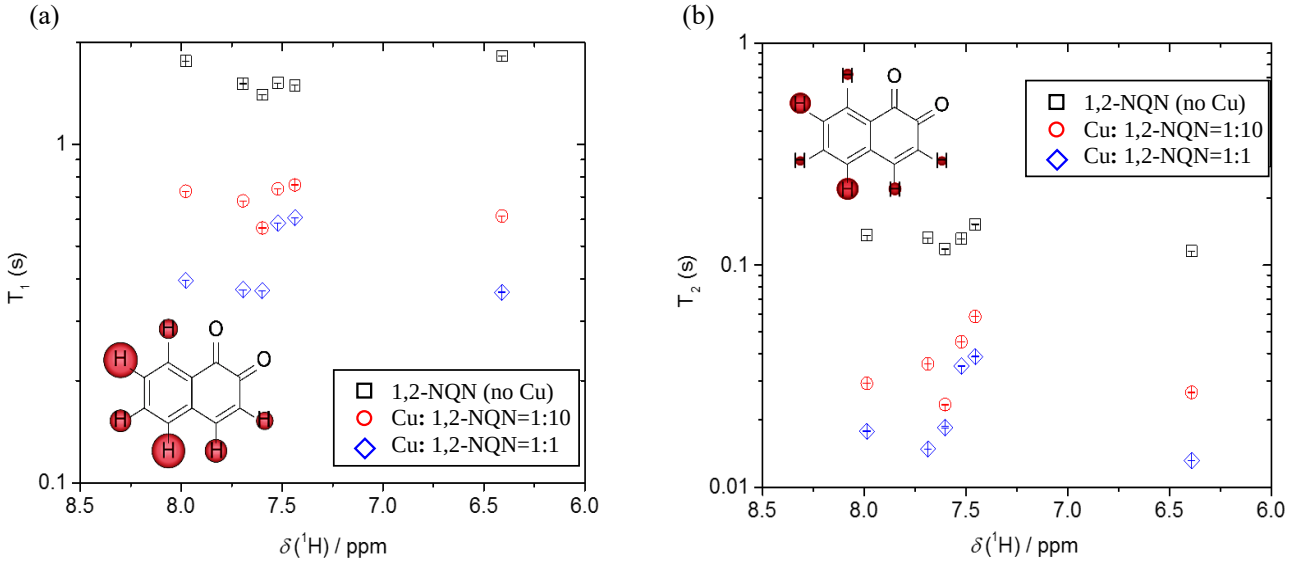

Figure 11. ^{1}H NMR relaxometry analyses for (a) T1, (b) T2 of 1,2-NQN mixed with Cu (II) at different ratios: 1,2-NQN with no Cu (**black**),Cu(II):1,2-NQN = 1:10 (**red**), Cu(II):1,2-NQN =1:1(**blue**). Both T1, T2 decreased when Cu was introduced into the system, indicating a smaller scale of nuclear spin dynamic resulted from organic-metal binding. The molecular epitopes illustrate the influence of Cu (II) binding on individual proton. A smaller sphere shadow on a proton denotes a larger relaxation influence from Cu (II)-organic binding.